Ain Shams Engineering Journal 15 (2024) 102548

Contents lists available at ScienceDirect

Ain Shams Engineering Journal

journal homepage: www.sciencedirect.com

To determine the compressive strength of self-compacting recycled aggregate concrete using artificial neural network (ANN)

Jesús de-Prado-Gil [a,*], Rebeca Martínez-García [b,*], P. Jagadesh [c], Andrés Juan-Valdés [d], María-Inmaculada Gónzalez-Alonso [e], Covadonga Palencia [a]

[a] Department of Applied Physics, University of León, Campus of Vegazana s/n, 24071 León, Spain
[b] Department of Mining Technology, Topography, and Structures, University of León. Campus of Vegazana s/n, 24071 León, Spain
[c] Department of Civil Engineering, Coimbatore Institute of Technology, Tamil Nadu 638 056, India
[d] Department of Agricultural Engineering and Sciences, University of León, Avenida de Portugal 41, 24071 León, Spain
[e] Department of Electrical Engineering and Systems and Automation, Campus de Vegazana s/n, University of León, 24071 León, Spain

A R T I C L E I N F O

Keywords:
Self-compacting concrete
Artificial neural network
Compressive strength
Recycled aggregate

A B S T R A C T

Nowadays, special concrete-like self-compacting concrete (SCC) requires sustainability by introducing recycled aggregates as a partial replacement for natural aggregate. Technological development initiatives in the construction sector estimate the 28 days' concrete compressive strength before casting due to faster requirement; one method selected is an artificial neural network. From works of literature, 515 mixed design are collected and utilized for training, validation, and testing data to prepare models. Different applications of SCC require different strengths of concrete. Based on control mix compressive strength, the mix designs are grouped into three families as low, medium, and high strength, apart from a common family. The correlation between input and output variables for three different families is analyzed. ANOVA analyses are done for input parameters. Coefficient of relation (R^2) is used for sensitive assessment and results for family I ($R^2 = 0.9299$), family II ($R^2 = 0.824$), family III ($R^2 = 0.8775$), and family IV ($R^2 = 0.7991$). Two further sensitivity analyses indicate that input parameters' influence varies for different families.

1. Introduction

A large amount of waste is generated in construction and demolition waste (C&DW) worldwide; therefore, many researchers have focused on the importance of its good management, especially in the case of waste from building demolition or debris, which represents 70–90 % of the total waste in general [1]. Due to the scarcity of land, demolishing city buildings is indispensable for carrying out new constructions [2,3]. However, it cannot be ignored that C&DW waste is widely known for the damage it can cause to the environment [3–6], thanks to the activities that originate it and promote the consumption of a large number of natural resources, energy, and emission associated with it [7,8]. Many researchers consider that the problems related to C&DW waste are not so much because its volume is hazardous when it occupies landfills; much of its content is non-hazardous and inert [9]. The utilization of CDW waste has been divided into three groups: management approaches or qualitative analysis, quantified modeling, and technical analysis. The former is control-oriented, including proposal management procedures, evaluation of the impacts of strategies, and construction-related determinants[10,11]. The opposite is true for quantified modeling, which encompasses more statistical and mathematical programming to assess the generation or social impact of construction and demolition waste. Finally, technical-analytical methods focus on the physical and mechanical properties of CDW waste and the development of reuse or recycling techniques or processes from a technical point of view [12,13]. According to studies related to quantified modeling, much attention should be paid to the usage of such waste in recycling processes. However, very little research has been devoted to predicting future waste generation and utilization, which is indispensable for its regulation [14,15]. Measures concerning C&DW waste should be proposed to be implemented in the long term to prevent or solve the waste problem in advance.

Song et al., 2016 [9] used a statistical method and Artificial Neural Networks (ANN) to predict information on the quantities and trends

* Corresponding authors.
E-mail addresses: jesusdepradogil@gmail.com (J. de-Prado-Gil), rmartg@unileon.es (R. Martínez-García), andres.juan@unileon.es (A. Juan-Valdés), inmaculada.gonzalez@unileon.es (M.-I. Gónzalez-Alonso), c.palencia@unileon.es (C. Palencia).

https://doi.org/10.1016/j.asej.2023.102548
Received 17 May 2023; Received in revised form 12 October 2023; Accepted 19 October 2023
Available online 28 December 2023

applicable to the utilization of CDW waste. Among the recycled materials obtained from CDW, the most common material is recycled coarse aggregate (RCA) and fine recycled aggregate (RFA) based on the size of materials recovered. Extensive studies are available on using these materials in concrete/mortar. Even sometimes, the combination of materials is also studied by several researchers. Aggregates comprise about 65–80 % of the concrete volume and are essential for several properties of concrete, such as mechanical and durability [16]. Large waste can be avoided by reusing recycled materials in concrete, solving several problems like environmental destruction, waste disposal, and pollution. While in this study, RCA and RFA are commonly referred to as recycled aggregate (RA). It is known that the incorporation ratio of the RA essentially conditions the compressive strength of RA. However, this ratio must be cautiously evaluated to improve the design of building applications. The compressive strength of concrete is directly related to the strength of aggregates used in the mix proportions. Introducing self-compacting concrete (SCC) to the market increased the interest in studying and optimizing the distribution and orientation of its improved rheological properties [17]. This concrete mix typically contains 100 % RCA and varying amounts of RFA, between 0 and 100 %, which would be tested for statistical analysis of their strength variations. The concrete industry is usually very modest; they have restricted resources to design the optimal mix for the concrete, the supply for usage of recycled coarse aggregates in self-consolidating concrete is scarce, and a limited number of literatures has been available for the past two decades. Compressive strength is one of the favorable characteristics of concrete used to assess its quality [18]. The number of samples required to calculate the compressive strength from experiments may increase due to experimental error. Researchers introduced the usage of RA in SCC to reduce the negative impacts produced by RA. The laboratory should investigate several mixes to obtain the desired 28 days of compressive strength with suitable workability. The number of samples needs materials, energy, cost, and waste generated after testing the models [4,18]. Besides, producing samples and the minimum curing period require more time [4].

The compressive strength of SCC is more sensitive to mix proportions and depends on several parameters; more enhanced approaches should be employed to reduce the necessity for experimental tests and afford expertise with more straightforward methods and mathematical formulas for forecasting experimental outcomes [16]. For the past decade, it has been widely accepted that applying ANN in civil engineering solves many problems [19].

Therefore, we need to progress an artificial model to project the compression strength of self-consolidating concrete using the artificial neural network. One such method focused on this study is the ANN, one of the extensively used primaries of all machine learning methods. By understanding the relationship amid the concrete composition and compression strength, we can better understand the concrete's nature and how to optimize the concrete mixture. Ji et al., 2006 [20] stated that the potential method to determine the compressive strength is ANN in terms of accuracy and efficiency when contrasted to models based on traditional and regression analysis approaches [21]. The high competence of the ANN makes it an appropriate tool when the connection between the inputs and output variables is not clear [22]. ANN is used in predicting the concrete properties [22,23], detecting the structure damage [24], structure system identification [25], materials behavior modeling [26,23], and creation of flowable concrete mixture models [27]. A sensitivity analysis was performed to assess the impact of the input variables on the output variables of mode. The sensitive analysis contains a list of approaches to measure how the uncertainty in the output of a model is linked to uncertainty in its inputs. In general, the sensitive analysis evaluates how sensitive the model is to instabilities in the parameters and data on which it is constructed. Sensitivity analysis results can have significant suggestions at many phases of the modeling process, including for finding errors in the model itself, notifying the standardization of model parameters, and reconnoitering more broadly the relationship between the inputs and outputs of the model [28].

Different structures require different strengths based on the applications [34]. A lot of literature is available concerning the effect of concrete strength on the properties of concrete. Several relationships exist in literature and standards concerning several properties (like modulus of elasticity, modulus of rupture, void size, etc.) to the strength of concrete. Even in literatures, the relationship between the advanced properties of SCC like compressive strength and fracture toughness [35,36] and the compressive strength and fracture energy [37] are reported. The introduction of new materials or new waste materials is affected by the strength properties and the properties based on strength. Hence, it is necessary to classify the strength of concrete as low, medium, and high based on the 28th day compressive strength on standard specimen size. It is a well-known fact that the strength of concrete purely depends on the ingredients used for the mix, as stated by standards and in literature. Different strength of concrete has different mix proportions, and the influence factors mainly depend on the proportion of mixtures. Hence, in this study, the mixed ingredients are considered for model development, and no other factors are included in developing the model. As stated in Table 1, apart from mix ingredients, several factors like water to cement ratio, size of recycled aggregates, water absorption characteristics of recycled aggregate, etc., play a minor role while designing mix proportions; it is not considered in this study.

Widespread usage of RA in the SCC has been noted from the last decade onwards; studies regarding the compressive strength prediction of SCC with RA are scary. Furthermore, the construction industry's growing desire for innovative buildings with unique characteristics to extend the service life of structures necessitates the development of creative models for forecasting. From the above discussion, it could be understood that ANN model for projecting compression strength from ingredients of self-consolidating concrete with recycled coarse aggregates could be developed. So, to the best of the author's knowledge and based on the past researches, there are no considerable studies that addresses the prediction of compressive strength from SCC ingredients with RA based on strength by utilizing ANN. And also, this study aims to make an equation to project the 28-day compressive strength of self-consolidating concrete ingredients, including recycled coarse aggregates. Finally, the objective of this study concludes with the sensitive assessment and sensitivity analysis for the model developed from ANN and ANN-based equations.

2. Material and methodology

2.1. Gathering of data points

In the present study, five hundred and fifteen data-points were collected from self-consolidating concrete with recycled coarse aggregates, which will be used for model development. Based upon the compression strength of the reference mixture, the data sets are grouped into four families, including a common family (Group IV), as tabulated in Table 2. Most of concrete applications are depending upon the compressive strength as governing factor. This compressive strength of concrete depends on the ingredients used to prepare it. Most of international standards and in literatures, the compressive strength of concrete is defined as high strength concrete, medium strength concrete and low strength concrete depending on the compressive strength. The classification of concrete strength is essential to ensure that the right type of concrete is used for particular construction project, taking into consideration for several factors such as applied load, project budget, specific requirement of structure, etc., Hence, in this study a method is proposed to divide the mix ingredients based on compressive strength for ease of their application purpose and also a common group to understand the difference between them.

Even in each family, there are sub-groups based upon the variation that occurs due to a replacement or additional percentage of recycled aggregates and also to take in admixture or binder content. Data points

Table 1
Summary of literature to estimate the compression strength of self-consolidating concrete, SCC with recycled aggregates, and RA concrete using ANN.

Author	Concrete	Method	Input Variables	Output variables	Data
Saha et al., 2017 [19]	Self-compacting concrete with recycled aggregates	ANN	Cement (kg), sand(kg), coarse aggregate (kg), fine aggregate (kg), fiber, water, superplastizer, viscous modifying agent	Compressive strength	99
Boudali et al., 2021 [29]	SCC with RAs	ANN	Binder (kg/m^3), Water/binder ratio, natural coarse aggregate (kg/m^3), recycled coarse aggregates (kg/m^3), natural pozzolan (kg/m^3), fly ash (kg/m^3), fine recycled concrete powder (kg/m^3), natural fine aggregate (kg/m^3), curing time (days)	Compressive strength (MPa)	240
Pazouki & Pourghorban et al., 2021 [19]	Self-compacting concrete with recycled aggregate	ANN	Cement (kg/m^3), water (kg/m^3), recycled coarse aggregate (kg/m^3), natural fine aggregate (kg/m^3), natural coarse aggregate (kg/m^3), binder (kg/m^3), age of specimen (days)	Compressive strength (MPa)	142
Asteris et al., 2016 [30]	Self-compacting concrete	ANN	Limestone powder (kg), fly ash (kg), GGBS (kg), Cement (kg), Silica fume (kg), RHA (kg), coarse aggregate (kg), fine aggregate (kg), water (kg), SP (kg), viscous modifying agent (kg)	Compression strength (MPa)	113
Faraj et al., 2019 [16]	Self-compacting concrete with recycled aggregates	ANN	Cement (kg/m^3), limestone powder (kg/m^3), fly ash (kg/m^3), silica fume (kg/m^3), GGBFS (kg/m^3), water to binder ratio, curing time (days), superplastizer (kg/m^3), recycled aggregates (kg/m^3), fine aggregate (kg/m^3), coarse aggregate (kg/m^3)	Compressive strength (MPa)	400
Morales et al., 2021 [31]	Recycled aggregate concrete	ANN	Cement (Kg/m^3), Fine aggregate (Kg/m^3), Water (kg/m^3), Superplastizer (kg/m^3), Fine Natural Aggregate (kg/m^3), Coarse Natural aggregate (kg/m^3), Recycled coarse aggregate (kg/m^3), Fineness modulus of fine natural aggregates, water absorption (%), density (kg/m^3)	Compressive strength (MPa)	177
Vasanthalin & Kavitha., 2021 [32]	Recycled aggregate concrete	ANN	Water to cement ratio, replacement percentage of recycled coarse aggregate, fine aggregate, natural coarse aggregate, recycled coarse aggregate, water absorption	Compressive strength (MPa)	121
Ridho et al., 2021 [33]	Recycled aggregate concrete	ANN	Cement (kg/m^3), blast furnace slag (kg/m^3), fly ash (kg/m^3), water (kg/m^3), superplasticizer (kg/m^3), coarse aggregate (kg/m^3), fine aggregate (kg/m^3), age (days)	Compressive strength (MPa)	1030
Yaman et al., 2017 [22]	Self-compacting concrete	ANN	Cement (kg/m^3), Fly ash (Kg/m^3), Water to powder ratio, sand (kg/m^3), coarse aggregate (kg/m^3), superplastizer (kg/m^3),	Compressive strength (MPa)	59

comprise of various limitations such as weight of sand, admixture, OPC, coarse aggregates, and water (kg/m^3), and the replacement ratio of recycled coarse aggregates (%) as output and input variables as 28 days compression strength. These limitations and their related data-points are separated into 3 elements [38,39] which will be discussed in the subsequent headings. The number of control mixes (based on compressive strength) in each family is plotted in Fig. 1. The histogram for compressive strength of different families for SCC with RA is shown in Fig. 2.

With the increase in the family, there is a reduction in the histogram of compression strength is noted in Fig. 2.

Normal distribution and frequency histogram analysis is the most commonly used statistical approach for reasonable quality control [79]. Fig. 3 show the histogram of various ingredients used in the mix preparation. Distribution of frequency for most of the families in the form of multimodal distribution. This indicates that the studies are coming from numerous dissimilar subpopulations. Hence, an attempt should be made to identify a moderating variable like the normalization of data that can explain the different effects of families. The weight of the histogram with mixed ingredients is varied by 50 kg/m^3 to find the corresponding frequency.

Fig. 3 (a) shows that the highest frequency is indicated for SP as 104. Next to SP, water has a frequency range of 5–51 with variations in weight as 150–300 kg/m^3. Fine aggregate has a frequency range of 1–25 with a weight variation of 600–1150 kg/m^3. Coarse aggregate has a frequency range of 1–25 with variations in weight as 450–to 1150 kg/m^3. Like family I, family II has the highest frequency for SP, as noted in Fig. 3 (b).

OPC has a frequency range of 1–43 with the variation of weight as 150–550 kg/m^3. Admixture has a frequency range of 6–54, with the weight variation as 0–400 kg/m^3. Water has a frequency range of 1–84 with the variation of weight as 150–300 kg/m^3. SP has a frequency range of 15–to 247, with the weight variation as 0–50 kg/m^3. Fine aggregate has a frequency range of 1–28 with a weight variation of 600–1175 kg/m^3. Coarse aggregate has a frequency range of 2–33 with various weights as 450–1175 kg/m^3 for family II as noted in Fig. 3 (b). Fig. 3(c) shows that family III also behaves similarly to family II and family I. Cement frequency of 2–30 is noted for family III with weight variation of 50–550 kg/m^3. Admixture has a frequency of 3–33 with various weights from 0 to 300 kg/m^3. Water has a frequency of 3–51 and is noted for variation in weight as 150–300 kg/m^3. Fine aggregate has a frequency of 1–26 and is indicated with a variation of weight as 700–1200 kg/m^3. Coarse aggregate has a frequency of 1–31 and is noted with a variation of weight as 550–1200 kg/m^3.

For family IV, the cement has a frequency range of 1–103 with the variation of weight as 100–650 kg/m^3. Admixture has a frequency range of 4–88 with a weight variation of 0–500 kg/m^3. Water has a frequency range of 1–160 with a variation in weight of 100–300 kg/m^3. The highest frequency is noted for SP in the field of 44–471, with variation in weight as 0–25 kg/m^3. Fine aggregate has a frequency range of 2–56 with variations in weight as 550–1200 kg/m^3. Coarse aggregate has a frequency range of 1–57 with a variation in weight of 475–1175 kg/m^3. Compared with other families, family IV has a slightly different histogram, as noted in Fig. 3(d).

2.1.1. Mandatory elements

In the present statistical research, mandatory elements comprise the compression strength (MPa) of the reference mixture at 28 days and different substitution ratios of natural aggregate by the recycled coarse aggregates (%), weight of sand, admixture, OPC, coarse aggregates, and water (kg/m^3), for different substitution ratios of natural aggregates by recycled coarse aggregates in the mixtures, the FA or CA is considered the sum of natural aggregate and their related recycled coarse aggregates. In few of the past researches, the rate of recycled coarse aggregates is evaluated from the substitution weight of natural aggregates directly. Thus, the weight per m^3 from mix design followed globally is measured as a mandatory elements [50].

2.1.2. Characteristic element

The properties of raw materials attained from the past researches like the binder's physical, chemical, and micro-properties, superplasticizer, and recycled coarse aggregate are not encompassed in the data points. As it is self-consolidating concrete of various grades, the chemical material is necessary such as high-range water reducing admixture, and

Table 2
Grouping of SCC with RA with respect to compression strength.

Family	Family compressive strength (MPa)	Control mix compressive strength (MPa)	Number of control mix	Number of the recycled aggregate mix	References
I	60 and above (High Strength Concrete)	72.47, 77.96 & 81.40	9	9	Gesoglu et al., 2015 [40]
		72.30	1	4	Wang et al., 2020 [41]
		74.10	1	5	Sadeghi-Nik., et al. 2019 [42]
		87	3	12	Khafaga., 2014 [43]
		60	1	4	Revilla Cuesta et al., 2020 [44]
		66.63	3	3	Gesoglu et al., 2015 [40]
		63.6	1	3	Fiol et al., 2018 [45]
		60.76	2	4	Behera et al., 2019 [46]
		62.2, 67.7	2	10	Ali et al., 2012 [47]
II	40 to 60 MPa (Medium Strength Concrete)	51.2	1	2	Señas et al., 2016 [48]
		50.4	1	4	Aslani et al., 2018 [49]
		58.3	1	3	Fiol et al., 2018 [45]
		57	1	7	Uygunoglu et al., 2014 [50]
		53.7	1	4	Kou et al., 2009 [51]
		52	1	5	Sadeghi-Nik., et al. 2019 [42]
		50	1	2	Grdic et al., 2010 [52]
		59	1	4	Tang et al., 2016 [50]
		52.3	1	3	Tuyan et al., 2014 [54]
		53.2	1	2	Kou et al., 2009 [51]
		52	1	4	Guneyisi et al., 2014 [55]
		59.85	1	5	Chakkamalayath et al., 2020 [1]
		58.2	1	2	Yu et al., 2014 [56]
		59.11	1	5	Zhou et al., 2013 [57]
		53.45	2	9	Guo et al., 2020 [58]
		55.7	1	4	Krishna et al., 2018 [59]
		54.2, 51.3	2	8	Khodair et al., 2017 [60]
		55.9	1	3	Katar et al., 2021 [61]
		47.6	1	2	Señas et al., 2016 [45]
		46.36	1	3	Martínez-García et al., 2020 [62]
		42.91	2	8	Duan et al., 2020 [63]
		45.6	1	5	Pan et al., 2019 [64]
		44.3	1	4	Kou et al., 2009 [51]
		43.8	1	3	Manzi et al., 2017 [65]
		46.3	4	6	Nili et al., 2019 [66]
		42.2	1	3	Tuyan et al., 2014 [54]
		42.34	4	8	Singh et al., 2019 [67]
		46.3	1	5	Ali et al., 2012 [47]
		49.09	1	3	Fiol et al., 2018 [42]
		43.40	1	3	Kumar et al., 2016 [68]
		48.51	1	5	Sharific et al., 2013 [69]
		44.3, 45.7	2	8	Khodair et al., 2017 [60]
		40.7, 42.81, 45.65, 42.65	4	16	Mahakavi and Chitra., 2019 [70]
III	Less than 40 MPa (Low Strength Concrete)	38.93	1	4	Aslani et al., 2018 [49]
		38.99	2	8	Bahrami et al., 2020 [71]
		35.5	1	4	Silva et al., 2016 [72]
		40.26	2	8	Sun et al., 2020 [73]
		36.66	1	6	Surendar et al., 2021 [74]
		37.2	1	3	Tuyan et al., 2014 [54]
		30.6	2	12	Babalola et al., 2020 [75]
		38.78	3	9	Nieto et al., 2019[76]
		36.2	1	4	Revathi et al., 2013 [77]
		36.5	1	3	Thomas et al., 2016 [78]
		33.79	1	4	Mahakavi and Chitra., 2019 [70]
		22.21	1	4	Aslani et al., 2018 [49]
		25.11, 24.78	2	8	Nieto et al., 2019 [76]

VMA for rheological and hard characteristics are found in most of the literature. Though high-range water reducing admixture's weight utilized in the mixture is significantly less, it has a significant part in the hardened characteristics of SCC [50].

2.1.3. Output elements (OEs)

The OEs measured in the present research is the compression strength of reference mixture of self-consolidating concrete with recycled coarse aggregates at curing of 28 days. The required factors considerably affect the compressive strength of self-consolidating concrete with recycled coarse aggregates. The past study confirms a firm relationship amid the mandatory elements and the compression strength of the traditional concrete.

2.2. Data processing

Data standardization is needed to map the source data into a targeted structural representation. It deals with the transformation of data-points

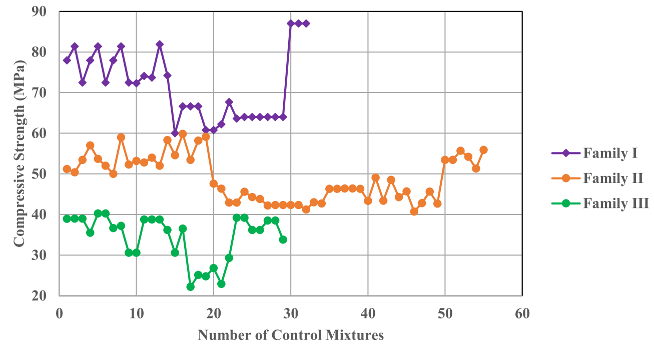

Fig. 1. Compressive Strength distribution of Control Mixture Proportions for SCC with RA.

after the data is gathered from different resources and prior to the analysis. Four different families are used for modeling, resulting in four other ANN models for projecting the compression strength of SCC with RA. The ANN model was performed in a MATLAB environment utilizing its embedded neural network toolbox. The input and output variables have been scaled between −1 and 1 using Eq. (1) to attain the dimensional consistency of the limits and eliminate the over-fitting of the trained network [80].

$$X_i = \frac{[2[X - X_{min}]]}{[X_{max} - X_{min}]} - 1 \quad (1)$$

Here X_i represents the standardised data, X_{max} represents the minimum value of X, X_{min} represents the higher value of X, and X signifies the empirical data. By employing the MS office, data standardization was carried.

2.3. Methodology

2.3.1. Data

To obtain estimates of the simplification error for the projecting models developed in the current study, every data set was separated into training and test sets. The data was separated into 75 % of all data points employed for training data and the remaining 25 % used for testing. The training data set was employed in every case to create the strength prediction models more suitable. In comparison, the testing data was employed only for final assessments of model performance.

2.3.2. Methodology

An artificial neural network is a method of artificial intelligence grounded on the brain's efficient aspect. The fundamental approach of the process of the artificial neural network is that it takes in the data through the neurons and input layer. Parameters such as weights and biases from the input layer to the hidden layer are generated randomly from a fixed domain and the weights at output are need to be calculated systematically [80 81,82]. In the unseen layer, the attained data is made to pass through the transfer function, which is generally nonlinear [83]. Then the output of the concealed layer is multiplied by the output weight before being fed to the output layer, passing through another transfer process known as feedforward. The difference between the experimental output and the projected output is calculated and is not equal to the predefined error function. The error function is proliferated backward, and the weights and biases are attuned till the predefined error function is fulfilled [84] .

The network property used for this model analysis is feedforward backpropagation. The training function used is TRAINLM, and the adaption learning function used is LEARNGDM. Properties of the hidden layer used are 1. The transfer function used for model analysis is TANSIG. The number of layers is varied depending upon the total number of variables (input and target variables), i.e., some hidden layers are varied up to 8 (strength {target variables}, cement, filler, fine aggregate, coarse aggregate, superplasticizer, percentage of RA and water {input variables}). Some of the layers used for the current study are being taken as eight initially, and the number of neurons varies up to 8. To determine the number of layers, the trial-and-error method was adopted by changing the number of neurons and layers, as shown in Table 3.

There were many specified empirical criteria for the number of neurons in the first hidden layer as a function of the number of input (N_i) and output (N_O) variables, as given in Table 4. And to find the number of neurons required for the current study, and from Table 4, the maximum number of neurons fixed for the trial-and-error method is 20, as tabulated in Table 5. To find an appropriate number of neurons, the number of layers is fixed as 1 and 2, as shown in Table 5.

2.3.3. Sensitive assessment

Parameters evaluated from models are very sensitive; a minor change in their value may lead to huge differences between the noted and projected values. Thus, for accurate simulated values prediction, the estimated parameters must be surely done to make the model accurate. Hence, for any statistical research, discovering sensitive parameters is highly considerable tasks [101] to judge the value similar to

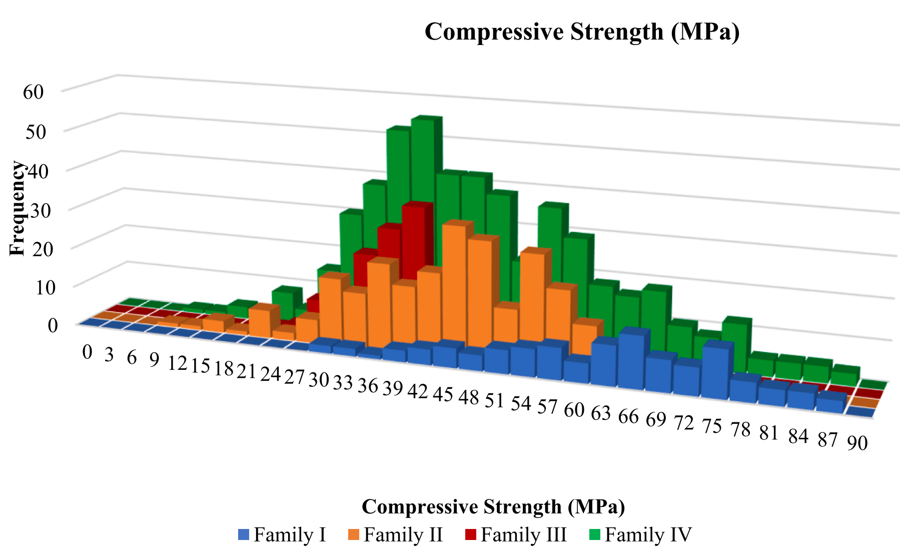

Fig. 2. Histogram of compressive strength for different families of SCC with RA.

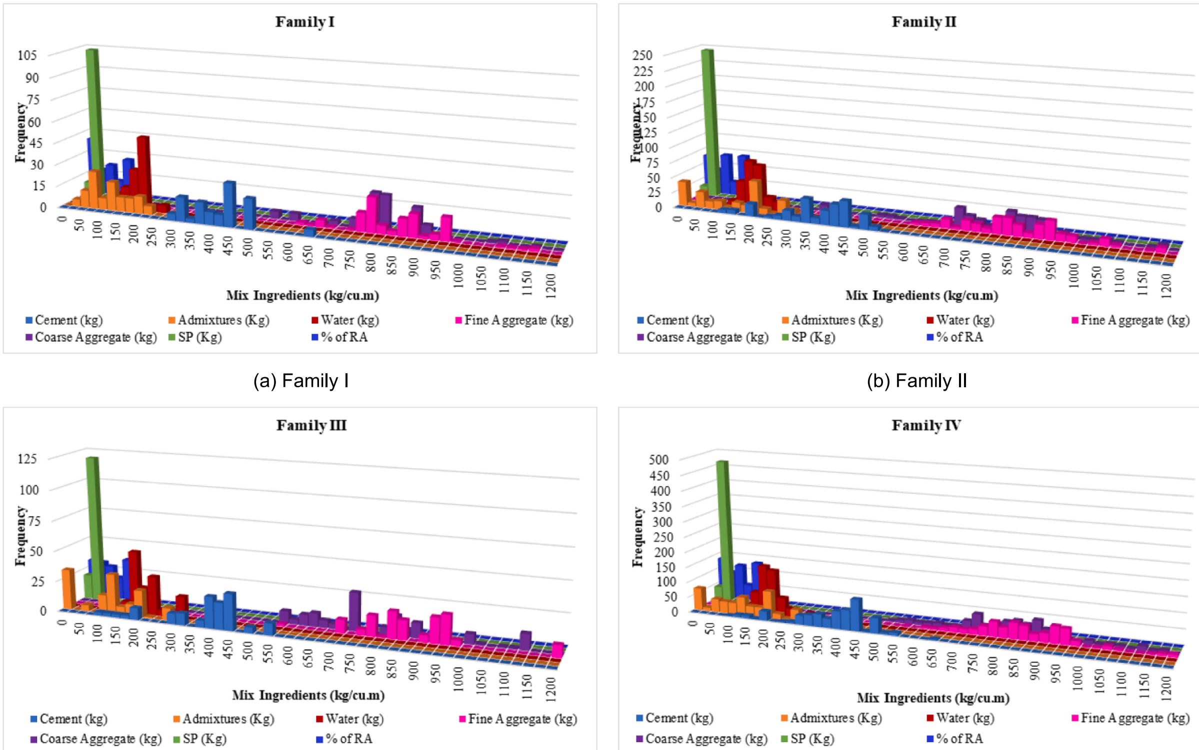

(a) Family I

(b) Family II

(c) Family III

(d) Family IV

Fig. 3. Histogram for mix ratio of ingredients for different families of SCC with RA.

Table 3
The number of hidden layers is constant, and the number of neurons varies.

Number of layers	Number of neurons
1	1, 2, 3, 4, 5, 6, 7, 8
2	1, 2, 3, 4, 5, 6, 7, 8
3	1, 2, 3, 4, 5, 6, 7, 8
4	1, 2, 3, 4, 5, 6, 7, 8
5	1, 2, 3, 4, 5, 6, 7, 8
6	1, 2, 3, 4, 5, 6, 7, 8
7	1, 2, 3, 4, 5, 6, 7, 8
8	1, 2, 3, 4, 5, 6, 7, 8

experimental results. In the current study, the sensitive assessment of the model predicted using the ANN coefficient of relationship (Equation (2)) is used.

$$\text{Coefficient of relation } R^2 = 1 - \frac{\sum (y_i - \hat{y}_i)^2}{\sum (y_i - \bar{y}_i)^2} \tag{2}$$

Here O_i is the observed value, P_i is the predicted value, N or n is the total no. of observed specimens, is the mean of the predicted value, p is the number of estimated regression coefficients, is the average of observed value, and is the average projected value.

3. Result and discussion

3.1. Correlation between output and input parameters

A co-relation between two variables is a number between −1 and + 1 exhibits the linearity of the relationship between variable [20]. More excellent linearity is noted when the value is close to + 1 [20]. The co-relation matrix is just a mathematical display of components' results on each other. Fig. 4 (a) exhibits that the compression strength strongly influences once on cement and has a lower impact on fine aggregate. The

Table 4
Summary of neurons in different hidden layers proposed in the literature.

Authors	Formulas	Values taken
Neville (1986) [85]	(3Ni/4)	6
Neville (1986) [85]	2Ni + 1	17
Hush., 1989 [86]	3Ni	24
Popovics., 1990 [87]	(Ni + No)/2	4.5
Gallant., 1993 [88]	2Ni	16
Wang., 1994 [89]	2Ni/3	5.6
Masters., 1994 [90]	$(Ni + No)^{0.5}$	3
Li et al., 1995 [91]	$[(1 + 8Ni)^{0.5} - 1]/2$	3.4
Tamura and Tateishi., 1997 [92]	Ni – 1	9
Lai and Serra., 1997 [93]	Ni	8
Nagendra., 1998 [94]	Ni + No	9
Zhang et al., 2003 [95]	$(2^{Ni}/Ni) + 1$	33
Shibata and Yuske., 2009 [96]	$(Ni \times No)^{0.5}$	2.3
Sheela and Deepa., 2013 [97]	$(4Ni^2 + 3) / (Ni^2 - 8)$	4.5
Hunter et al., 2012 [98]	$2^{Ni} - 1$	255
Ripely., 1993 [99]	(Ni + No)/2	4.5
Paola., 1994 [100]	$[2 + (No \times Ni) + 0], [5No (No^2 + Ni) - 3] / (No + Ni)$	1.2
Hunter et al., 2012 [98]	Log (Ni-1) - No	2

Table 5
The number of neurons is constant, and the number of hidden layers varies.

Number of layers	Number of neurons
1, 2	1, 2, 3, 4, 5, 6, 7, 8, 6, 7, 8, 9, 10, 11, 12, 13,14, 15, 16, 17, 18, 19, 20

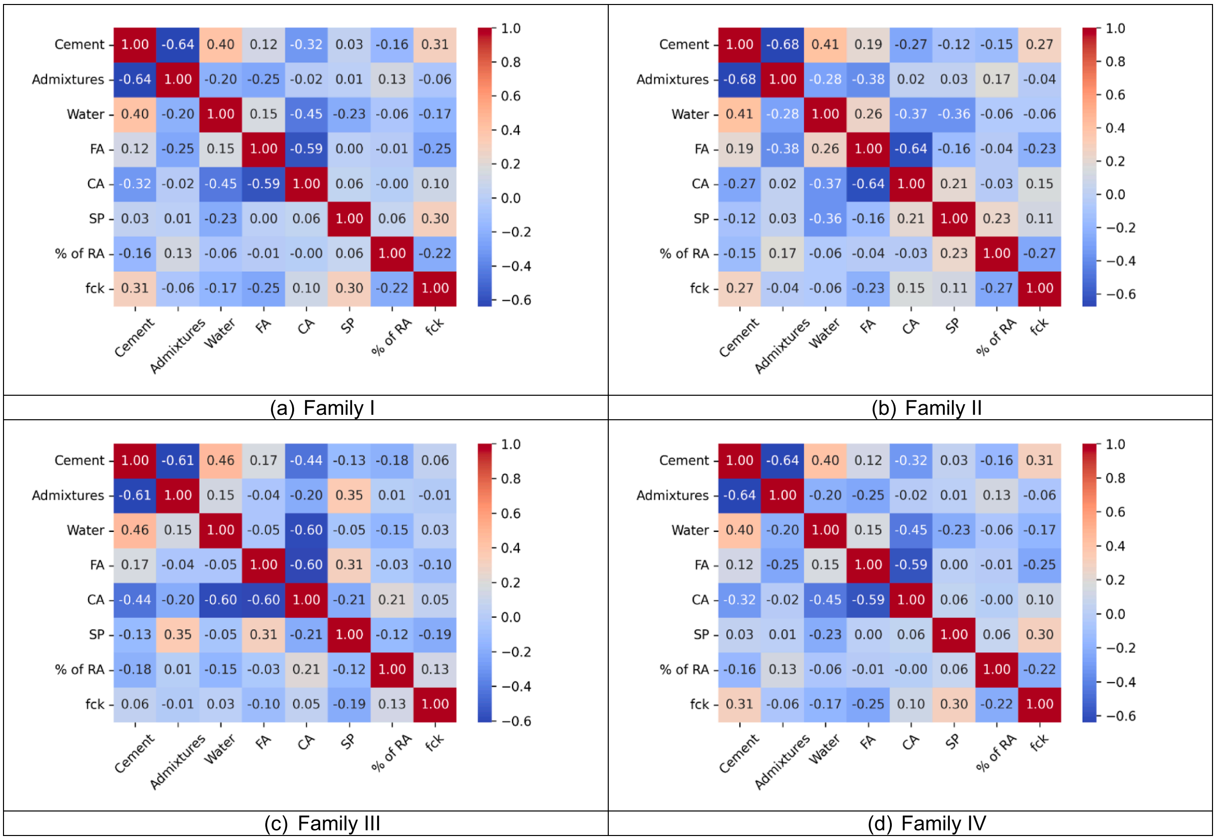

Fig. 4. Correlation matrix for different families of SCC with RA.

negative effect is observed in the order of fine aggregate, percentage of RA, water, and admixtures. The positive impact is kept in the order of cement, SP, and coarse aggregate. For family II, compression strength has a more substantial impact on cement, and a lesser impact on the percentage of recycled aggregate is noted in Fig. 4 (b). The negative effect is stated in the order of percentage of RA, fine aggregate, water, and admixtures. The positive impact is observed in the order of cement, coarse aggregate, and SP. For family III, compression strength has a high positive impact on percentage of RA and negative impact on SP is noted from Fig. 4 (c). Negative influence is observed in the order of SP, fine aggregate and admixtures. Positive influence is observed in the order of percentage of RA, cement, coarse aggregate and water. Positive and negative influence varies concerning different mixed ingredients is noted. Typical ingredients for positive impact are cement, and negative impact is fine aggregates and admixtures. A Spearman correlation to determine the association of compressive strength and mixed ingredients with each other, as observed in Fig. 4. Revilla-Cuesta et al., 2020 [20] noted similar negative and positive influences of input variables on compressive strength (output variable).

From Fig. 4(a), it is noted that there is highest positive relationship is noted between the cement and water. Whereas the highest negative relationship between the cement and admixtures for family I. Similarly for family II (Fig. 4(b)), family III (Fig. 4(c)) and family IV (Fig. 4(d), same kind of positive relationship and negative relationship are observed. The highest negative relationship is noted for family II and the lowest negative relationship is noted for family II, whereas for highest and lowest positive relationship between is noted for family III.

From Fig. 4(c), it is noted that there is highest positive relationship between the cement and water, whereas the lowest relationship between the cement and admixture for family III. For family IV, from Fig. 4(d), the highest positive relationship between the cement and water, whereas the lowest Analysis of variance.

3.2. Analysis of variance of input parameters

Analysis of variance is performed for the entire families to comprehend the influence of input on output limitations [53]. The p-value evaluates the suitability of diminishing the null hypothesis as a hypothesis test and ranges from 0 to 1. The smaller the p-value, the smaller the probability that is reducing the null hypothesis is an error. The t-value represents the significance of the regression coefficient. Higher the value of 't' and lower the value of 'p', indicates that the coefficient of term is more significant. For example, in Table 6, the lowest p-value is noted for the cement in Family IV, which indicates that the 't' is highest value. The alpha (α) level in this study was defined as 0.05. Thus, items in ANOVA with a p-value less than 0.05 are considered significant [45]. Much influencing parameter for the family I is in the order of cement, admixture, water, fine aggregate, SP, and percentage of RA. Whereas for family II, the much influence parameter is in the order of cement, admixture, coarse aggregate, SP, and percentage of RA. For family III, the much influencing parameter is noted as SP alone.

In contrast, family IV is in the order of cement, admixture, water, fine aggregate, SP, percentage of RA, and admixtures influence more. From Table 6, it can be concluded that the compressive strength directly depends on different types of ingredients for mix preparation. And also, depending on the grade of concrete, the ingredient chosen varies; for example, the higher the strength of concrete, the influence of all components (specifically cement, percentage of RA, SP, coarse aggregate, and fine aggregate) is more. In contrast, for the lower strength of concrete, the influence of each ingredient is reduced.

From Table 7, it is observed that the variation in compression strength variation depends on the input parameters used for each family. Much deviation of input parameters for each family is noted for cement, fine aggregate, and coarse aggregate. It is also stated that when the percentage of recycled aggregate replacement is less, the compressive strength is high. An increase in the fine aggregate results in increased

Table 6
Effect of input parameters on output parameters by employing analysis of variance.

Input Parameters	Family I		Family II		Family III		Family IV	
	t Stat	*P-value*	*t Stat*	*P-value*	*t Stat*	*P-value*	*t Stat*	*P-value*
Cement (kg)	6.585	1.8E−09	6.483	4.7E−10	1.966	0.051	9.073	2.552E−18
Admixtures (Kg)	2.683	0.008	3.545	0.0004	1.868	0.063	3.367	0.0008
Water (kg)	−4.023	0.00011	−1.104	0.270	−0.642	0.521	−6.00	3.752E−09
Fine Aggregate (kg)	−3.987	0.00012	−0.473	0.636	0.0866	0.931	−4.232	2.738E−05
Coarse Aggregate (kg)	−0.741	0.46	2.256	0.024	0.779	0.436	0.281	0.778
SP (Kg)	4.264	4.4E−05	2.626	0.009	−2.260	0.025	6.289	6.890E−10
% of RA	−4.547	1.5E−05	−5.008	1E−06	1.368	0.173	−5.220	2.61E−07

Table 7
Contribution of each input variable to output variable using ANOVA analysis.

Input Parameters	Family I		Family II		Family III		Family IV	
	SSQ	*% of contribution*	*SSQ*	*% of contribution*	*SSQ*	*% of contribution*	*SSQ*	*% of contribution*
Cement (kg)	20,146,061	11.637	37,254,439	8.912	20,749,355	9.268	78,149,855	9.588
Admixtures (Kg)	1,977,607	1.142	9,511,045	2.275	2,845,633	1.271	14,334,284	1.759
Water (kg)	3,259,892	1.883	8,083,544	1.934	5,456,139	2.437	16,799,575	2.061
Fine Aggregate (kg)	77,077,526	44.523	1.9E + 08	45.419	1.08E + 08	48.248	3.75E + 08	46.006
Coarse Aggregate (kg)	70,303,326	40.610	1.72E + 08	41.233	86,310,930	38.552	3.29E + 08	40.364
SP (Kg)	5783.13	0.003	7673.364	0.002	1971.943	0.001	15428.43	0.002
% of RA	347,450	0.201	943459.3	0.226	499,475	0.223	1,790,384	0.22

SSQ – Sum of Squares.

compressive strength observed among all the groups apart from the standard group. An increase in water results in a decrease in compressive strength is noted. Percentage of contribution for the compressive strength are in the order of fine aggregate, coarse aggregate, cement, water and admixture (higher to lower) for all the families are observed. An increase in SP results in an increase in compressive strength is observed. No constant relationship was pointed out between the compressive strength, cement, and admixture. Kelestemur et al., 2014 [102] observed the contribution of various factors to the compressive strength using ANOVA analysis.

3.3. Influence of number of layers on the predicted compressive strength

ANN architecture is explained as how many number layers a network has, the number of neurons in each layer, the activation function of each layer, and how the layers are connected. The selection of an optimum ANN architecture is an open problem of examination and depends on the application domain [103]. Several layers should be determined to get a better value in sensitive assessment [20,104].

The value of R^2 increases with the number of layers for a training set of the family I are noted in Table 8. But for testing, there is no strong relationship between the layers and the R^2 value. Layer 4 is the higher R-square values for training, and layer one is the higher R-square values for testing.

R^2 value decreases with an increase in several layers are noted for family II is observed from Table 9 shows no constant relationship between layers and R^2 value is indicated. It is observed that the higher R^2 value is noted for layer 1 for training and layer 2 for testing. Family I and family II is showing similar behavior. R^2 value increases with the increase in several layers are observed in Table 10 for family III, and testing the R^2 value shows no constant relationship between layer and R^2. For family IV, Table 11 indicates that the increase in the number of neurons increases R^2 is noted with training for layer 4, and testing for layer 1 shows that increase in the number of neurons san increases R^2.

Developing the ANN-based equation if the number of layers increases means the equation becomes more complicated. Hence, the number of layers is maintained at 2 for all families to reduce complications.

3.4. Influence of number of neurons on the predicted compressive strength

A significant problem in scheming a network is how many neurons are required in every concealed layer. Utilizing a lot of neurons could cause a flawed acknowledgment of signal in a complex underfitting or dataset. Using a lot of neurons raises the lattice time, maybe too much to train when it is implausible to train in a sensible amount of time. A lot of neurons can cause overfitting, in which case the network has a lot of data, or the quantity of material in the training set does not have enough exact information to train the network [108]. The most acceptable number of hidden units relies on several aspects—the number of outputs, inputs of the network, the number of cases in the data set, the intricacy of the error function, the noise of the target data, the architecture of the network, and algorithm of network training.

In most cases, there is generally no way to simply evaluate the optimized quantity of neurons in the concealed layer with no need to train the network [109]. The optimal method is to utilize the trial-and-error procedure to assess the number of neurons in every layer. It is probable to use the backward selection process to evaluate the number of units in the concealed layer. Progressive selection starts with selecting a rational rule for the performance assessment of the network. Afterward, a minor number of concealed units, trains, and tests are set to

Table 8
Influence of layers for the family I in terms of R^2 value.

	Training								Testing							
Neurons	1	2	3	4	5	6	7	8	1	2	3	4	5	6	7	8
Layer 1	0.65	0.69	0.73	0.80	0.83	0.84	0.86	0.88	**0.45**	**0.48**	**0.52**	**0.53**	**0.57**	**0.60**	**0.65**	**0.66**
Layer 2	0.64	0.69	0.74	0.80	0.85	0.87	0.89	0.90	0.31	0.39	0.46	0.50	0.54	0.59	0.63	0.66
Layer 3	0.65	0.72	0.74	0.81	0.85	0.91	0.90	0.86	0.20	0.23	0.25	0.27	0.35	0.46	0.58	0.47
Layer 4	**0.68**	**0.74**	**0.75**	**0.81**	**0.84**	**0.89**	**0.90**	**0.84**	0.26	0.29	0.30	0.34	0.37	0.51	0.63	0.56

Table 9
Influence of layers for family II in terms of R^2 value.

	Training								Testing							
Neurons	1	2	3	4	5	6	7	8	1	2	3	4	5	6	7	8
Layer 1	**0.52**	**0.55**	**0.60**	**0.63**	**0.67**	**0.72**	**0.75**	**0.79**	0.25	0.28	0.31	0.35	0.37	0.39	0.44	0.47
Layer 2	0.50	0.53	0.58	0.62	0.65	0.71	0.74	0.78	**0.27**	**0.31**	**0.35**	**0.43**	**0.49**	**0.53**	**0.57**	**0.58**
Layer 3	0.47	0.50	0.55	0.58	0.60	0.65	0.68	0.69	0.22	0.27	0.33	0.36	0.39	0.44	0.47	0.54
Layer 4	0.44	0.46	0.52	0.52	0.56	0.61	0.63	0.65	0.24	0.30	0.35	0.42	0.45	0.50	0.54	0.57

Table 10
Influence of layers for family III in terms of R^2 value.

	Training								Testing							
Neurons	1	2	3	4	5	6	7	8	1	2	3	4	5	6	7	8
Layer 1	0.38	0.44	0.53	0.57	0.65	0.73	0.76	0.80	0.52	0.59	0.65	0.69	0.72	0.75	0.76	0.79
Layer 2	**0.46**	**0.49**	**0.57**	**0.64**	**0.69**	**0.77**	**0.80**	**0.84**	0.47	0.55	0.60	0.65	0.69	0.73	0.76	0.79
Layer 3	0.40	0.45	0.54	0.59	0.66	0.73	0.78	0.81	0.50	0.58	0.63	0.68	0.73	0.76	0.78	0.81
Layer 4	0.43	0.49	0.56	0.62	0.69	0.77	0.82	0.84	**0.53**	**0.62**	**0.6**	**0.71**	**0.74**	**0.79**	**0.81**	**0.82**

Table 11
Influence of layers for family IV in terms of R^2 value.

	Training								Testing							
Neurons	1	2	3	4	5	6	7	8	1	2	3	4	5	6	7	8
Layer 1	0.75	0.77	0.80	0.82	0.83	0.86	0.88	0.92	**0.59**	**0.61**	**0.64**	**0.66**	**0.70**	**0.76**	**0.81**	**0.87**
Layer 2	0.78	0.82	0.84	0.87	0.88	0.90	0.92	0.96	0.55	0.58	0.63	0.66	0.69	0.73	0.79	0.83
Layer 3	0.80	0.84	0.85	0.89	0.89	0.92	0.93	0.96	0.58	0.60	0.66	0.69	0.73	0.78	0.82	0.86
Layer 4	**0.83**	**0.86**	**0.88**	**0.90**	**0.91**	**0.93**	**0.95**	**0.97**	0.56	0.58	0.64	0.68	0.71	0.76	0.79	0.85

assess the network's performance. Training and testing for the family I are increased with an increase in the number of neurons for both layers for R^2 value up to the 13th neuron; after that, it decreases, as shown in Table 12. Training and testing for family II are increased with an increase in the number of neurons for both layers up to the 11th neuron, and after that, it decreases.

Table 13 indicates the influence of neurons for family III and family IV. Similar to the family I and II, families III and IV show the same relationship. Testing and training for families III and IV increase with the number of neurons up to the 12th neuron and 9th neuron.

Tables 12 and 13 show that the number of neurons in each layer for a model depends on several variables used for the model. And also, it is worth mentioning that the number of neurons used is less than 25, as used by several researchers in Table 3. Expect few researchers who used too many neurons for their models to develop the ANN model. To create a mathematical equation based on ANN, the number of neurons used should be minimized as much as possible to avoid complexity. Jiang et al., 2021 [107] trained and tested many datasets to optimize the number of neurons selected for their problem statement. Optimized architecture is determined based on the results of the sensitive assessment. The number of neurons used in each layer is evaluated by the trial and error process by Tavakoli et al., 2014 [23] and Mashhadban et al.,

Table 12
Influence of neurons for the family I and family II in terms of R^2 value.

Neurons	Family I				Family II			
	Training		Testing		Training		Testing	
	Layer 1	Layer 2	Layer 1	Layer 2	Layer 1	Layer 2	Layer 1	Layer 2
1	0.65	0.64	0.45	0.31	0.52	0.50	0.31	0.27
2	0.69	0.69	0.48	0.39	0.55	0.53	0.35	0.31
3	0.73	0.74	0.52	0.46	0.60	0.58	0.40	0.35
4	0.80	0.80	0.53	0.50	0.63	0.62	0.47	0.43
5	0.83	0.85	0.57	0.54	0.67	0.65	0.53	0.49
6	0.84	0.87	0.60	0.59	0.72	0.71	0.55	0.53
7	0.86	0.89	0.65	0.63	0.75	0.74	0.59	0.57
8	0.88	0.90	0.66	0.66	0.79	0.78	0.63	0.58
9	0.90	0.92	0.69	0.68	0.82	0.81	0.67	0.64
10	0.91	0.93	0.73	0.70	0.84	0.83	0.71	0.67
11	0.92	0.94	0.78	0.74	**0.86**	**0.83**	**0.77**	**0.73**
12	0.93	0.95	0.83	0.78	0.82	0.77	0.75	0.71
13	**0.95**	**0.97**	**0.86**	**0.82**	0.78	0.73	0.66	0.62
14	0.92	0.94	0.82	0.76	0.76	0.69	0.59	0.56
15	0.91	0.93	0.76	0.63	0.73	0.65	0.56	0.49
16	0.89	0.91	0.74	0.57	0.72	0.62	0.53	0.44
17	0.88	0.88	0.62	0.36	0.68	0.57	0.47	0.39
18	0.88	0.86	0.47	0.32	0.65	0.54	0.45	0.32
19	0.87	0.82	0.37	0.22	0.62	0.50	0.33	0.28
20	0.85	0.78	0.22	0.14	0.58	0.48	0.15	0.18

Table 13
Influence of neurons for family III and family IV in terms of R^2 value.

Neurons	Family III				Family IV			
	Training		Testing		Training		Testing	
	Layer 1	Layer 2	Layer 1	Layer 2	Layer 1	Layer 2	Layer 1	Layer 2
1	0.38	0.46	0.52	0.47	0.75	0.78	0.59	0.55
2	0.44	0.49	0.59	0.55	0.77	0.82	0.61	0.58
3	0.53	0.57	0.65	0.60	0.80	0.84	0.64	0.63
4	0.57	0.64	0.69	0.65	0.82	0.87	0.66	0.66
5	0.65	0.69	0.72	0.69	0.83	0.88	0.70	0.69
6	0.73	0.77	0.75	0.73	0.86	0.90	0.76	0.73
7	0.76	0.80	0.76	0.76	0.88	0.92	0.81	0.79
8	0.80	0.84	0.79	0.79	0.92	0.96	0.87	0.83
9	0.83	0.87	0.80	0.82	**0.97**	**0.99**	**0.94**	**0.89**
10	0.85	0.89	0.84	0.85	0.94	0.94	0.93	0.89
11	0.88	0.91	0.86	0.89	0.91	0.90	0.89	0.85
12	**0.94**	**0.97**	**0.89**	**0.93**	0.88	0.88	0.86	0.80
13	0.93	0.92	0.92	0.95	0.86	0.84	0.83	0.77
14	0.88	0.87	0.89	0.90	0.83	0.79	0.78	0.73
15	0.87	0.83	0.82	0.83	0.79	0.76	0.75	0.68
16	0.84	0.78	0.79	0.79	0.76	0.71	0.72	0.64
17	0.78	0.73	0.73	0.74	0.73	0.67	0.68	0.58
18	0.73	0.67	0.65	0.67	0.71	0.64	0.65	0.55
19	0.66	0.61	0.59	0.57	0.68	0.60	0.62	0.53
20	0.56	0.51	0.53	0.51	0.66	0.56	0.58	0.46

2016 [104]. The influence of neurons on output variables is confirmed by Tavakoli et al., 2014 [23], and the best model is selected based on sensitive assessment.

3.5. Predicted compressive strength using ANN

Compressive strength predicted from the trained ANN network for family I to family IV is shown in Fig. 5. Family, I indicate that the higher compressive strength shows a higher R^2 value among all the families, whereas the lower R^2 value is family IV.

Fig. 6 compares experimental readings and the predicted strength value for each family. The family I show similar predicted compressive strength as experimental strength. Next to family I, family III shows similar predicted compressive strength as experimental strength. The lowest prediction is observed for family IV. The Box plot for all families is shown in Fig. 7. Predicted compressive strength for family IV and experimental compressive strength show similar values. Family III offers lower and higher predictions for the family I for predicted and experimental compressive strength. Machine learning for SCC in literature is shown in Table 14. ANN shows better results based on sensitive assessments for SCC is noted.

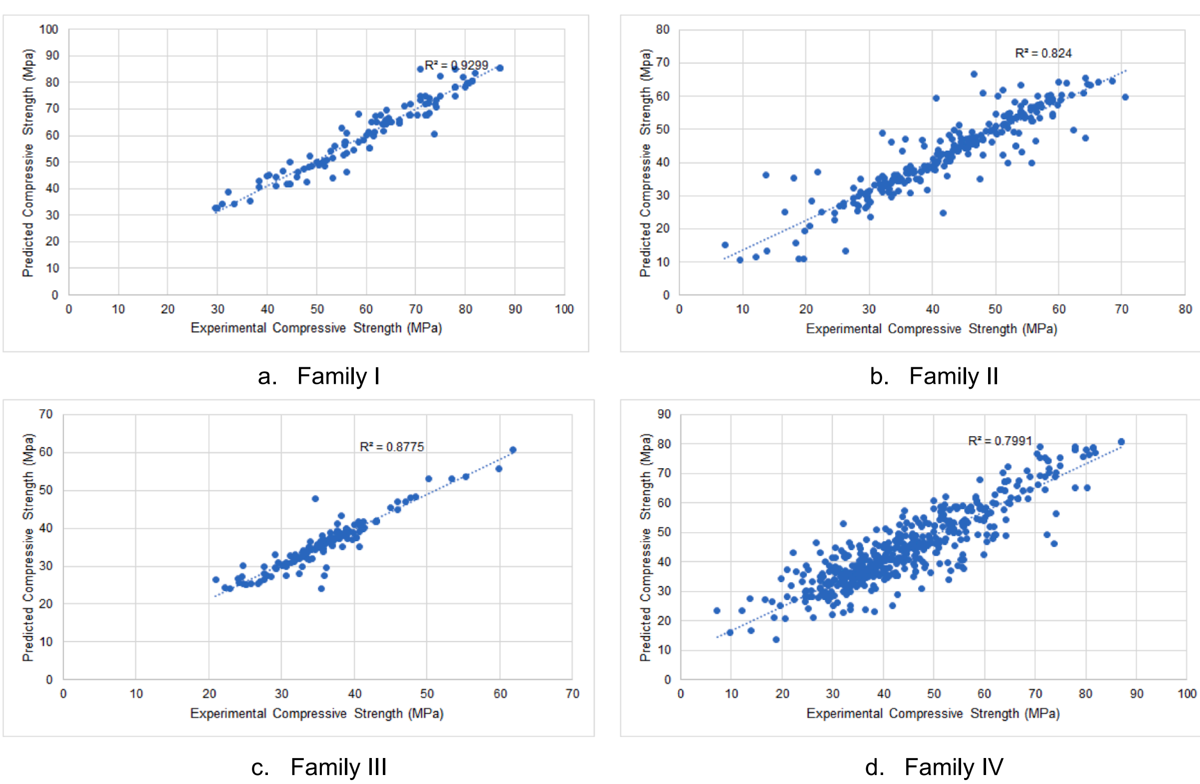

Fig. 5. Predicted and experimental compressive strength (MPa) for SCC with RA.

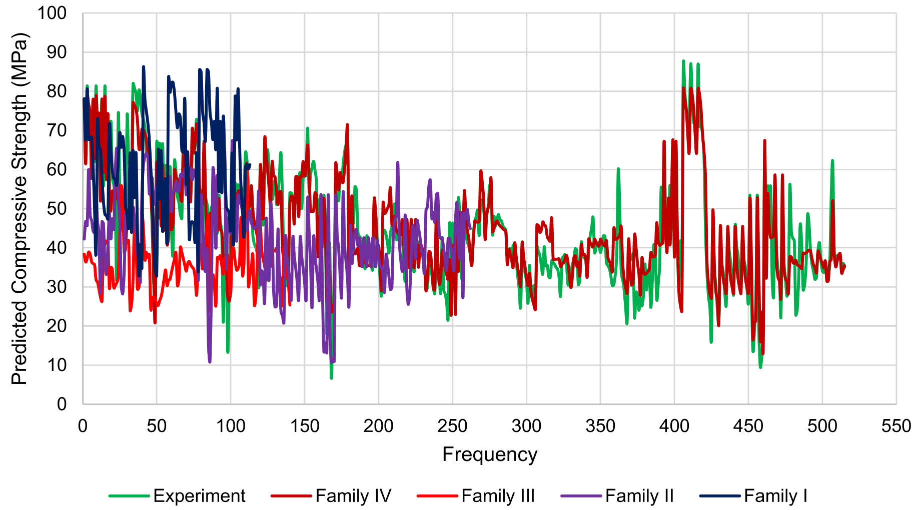

Fig. 6. Comparing experimental compressive strength to predicted compressive strength using various statistical tools from raw data.

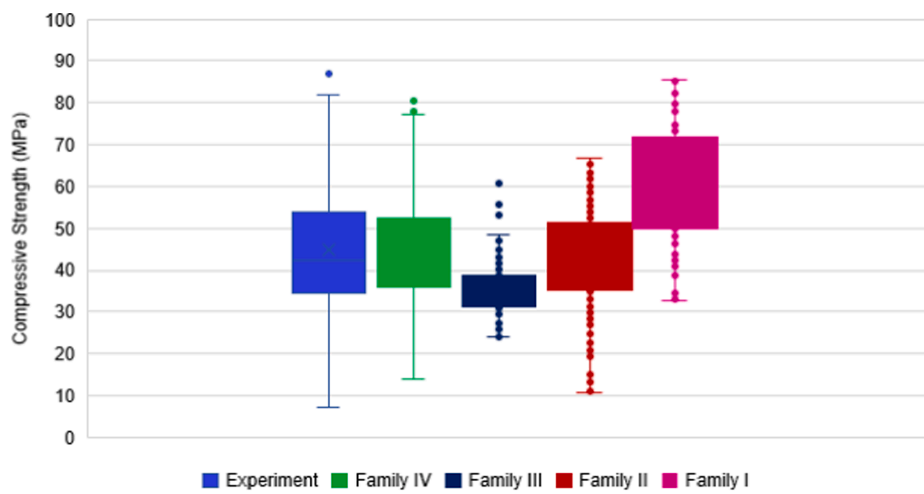

Fig. 7. Box plot of experimental and predicted compressive strength.

Table 14
Summary of model performance of SCC from literature using ANN.

References	Method	Number of input parameter	Number of the Output parameter	Number of Data	Model performance
Aggarwal and Aggarwal., 2011[108]	ANN	6	1	60	RMSE = 5.557 MAE = 4.438
Awoeyera et al., 2020 [109]	ANN	9	3	412	R^2 = 0.93
Tavakoli, et al., 2014 [23]	Feed forward multi-layer perceptron (MLP) sort of ANN	2	3	28	–
Mashhadban et al., 2016 [104]	Particle Swarm Optimization Algorithm, PSOA integrated with ANN	3	4	–	RMSE = 0.037 RMSE = 0.011
Uysal et al., 2012 [110]	ANN feed forward back propagation	11	1	85	R^2 = 0.95
Prasad et al., 2009 [111]	ANN with back propagation	10	1	300	R^2 = 0.91
Yeh et al., 2007 [105]	ANN with Back Propagation network	7	1	78	R^2 = 0.78
Siddique et al., 2011 [112]	ANN with back propagation network ANN with back propagation network	6 (Cement, fly ash, water/powder, SP dosage, sand, coarse aggregate)	1 (compressive strength)	80	R^2 = 0.9187 R^2 = 0.9587

3.6. K Fold method to determine optimum ANN equation

To get optimized combination of dataset for training and testing purpose, the data's are divided into number of data subsets [82,113]. In present study, k-fold-cross validation, number of datasets (collected) are divided into ten subsets, which is used for training and testing of the data. The K fold cross validation method is used to determine the optimum weight to each layer and bias to each hidden layer. In this research paper, the K fold value is taken as 10, i.e., the training and testing value keeps changing to 10 times to get the best weight and bias value based on the coefficient of relation value [106].

Figs. 8 and 9 show the weight to layer and bias for all families in the

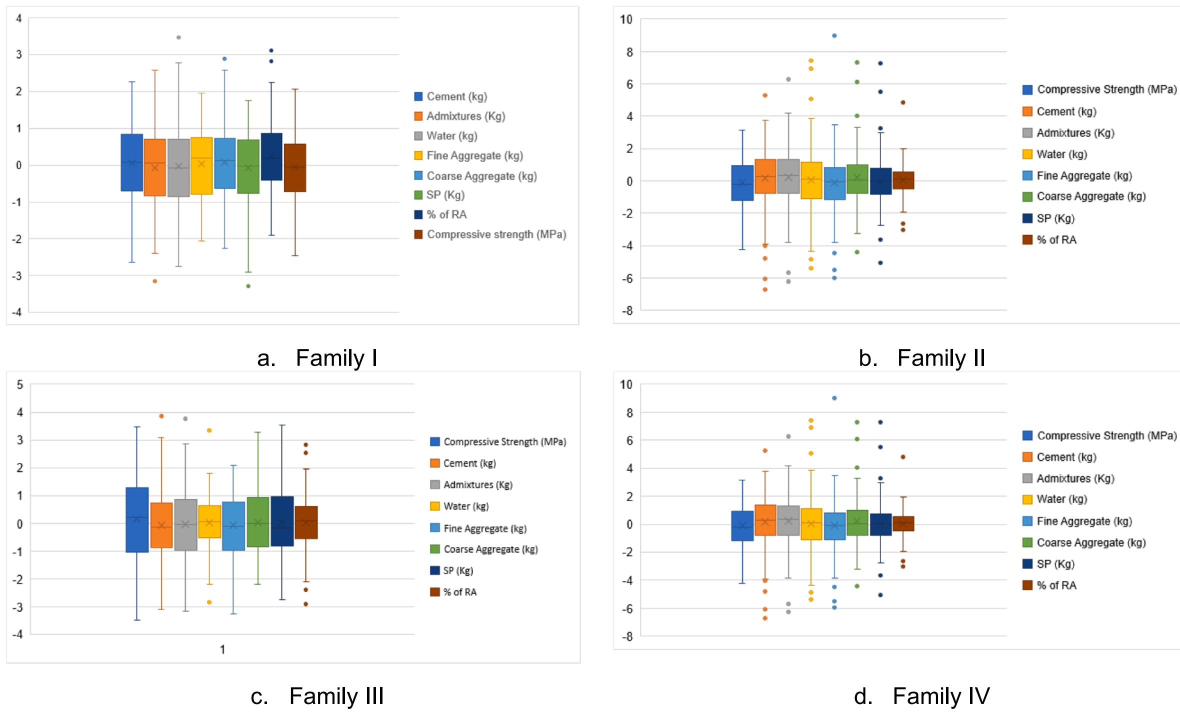

Fig. 8. K Weight to layer for the families (K fold).

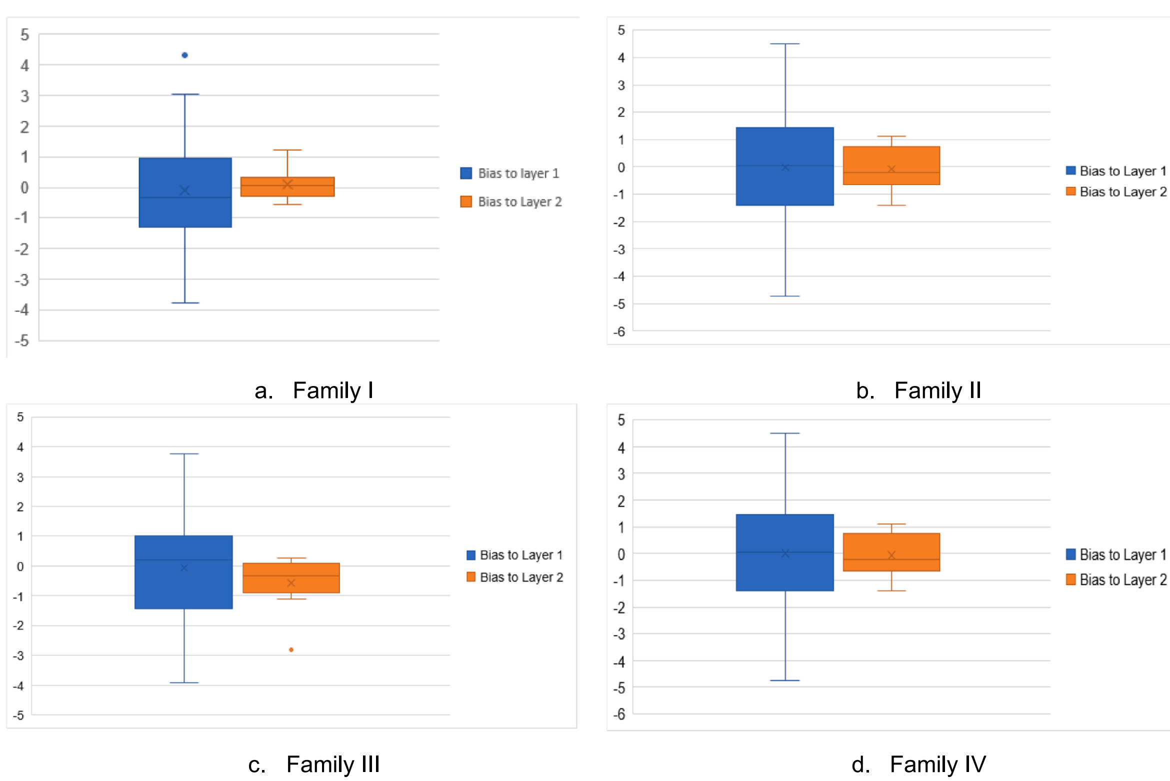

Fig. 9. K Bias to each layer for the families (K fold).

box plot. In training and testing, the best set is determined in Fig. 10. And their corresponding weights and bias for family I (K = 6) for Table 15 and Table 16 (K = 4) for family II. Family III and IV for Table 17 (K = 10) and Table 18 (K = 1).

3.7. Development of ANN-based formula for projecting the compressive strength

A qualified artificial neural network can be converted into a mathematical formula over the weights and the biases in combination with the transfer equation [89]. From Fig. 11, the predicted compressive

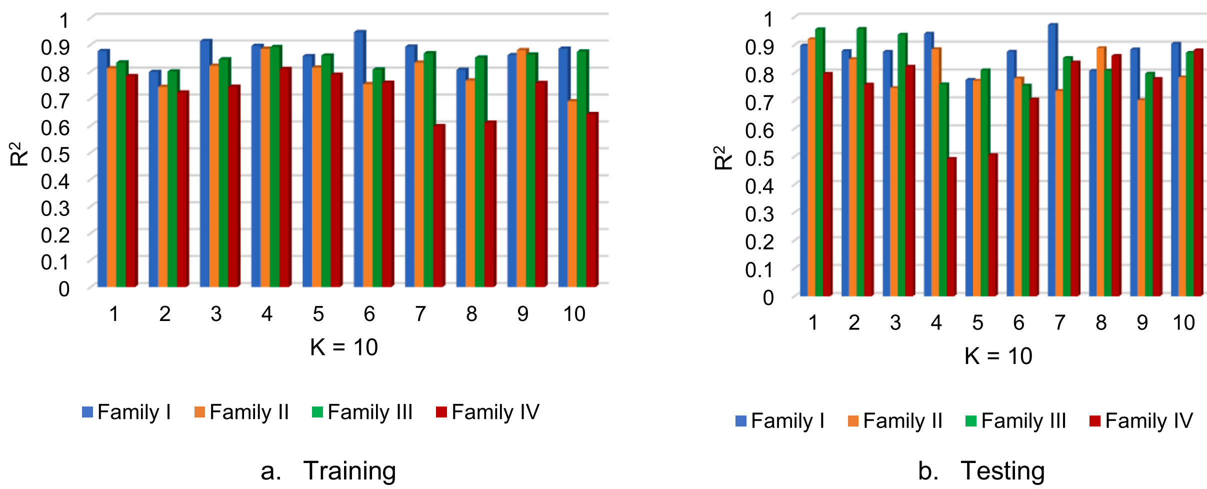

Fig. 10. K fold validation to determine the best fold.

Table 15
Weight and bias for a different family I for fold K = 6.

Neurons	Weight to								Bias to	
	fck (MPa)	C (kg)	A (Kg)	W (kg)	FA (kg)	CA (kg)	SP (Kg)	% of RA	Layer 1	Layer 2
	Wi	W1	W2	W3	W4	W5	W6	W7	B1	B2
1	−1.006	0.307	0.473	1.604	0.366	0.520	1.228	0.017	−1.191	0.276
2	0.321	−0.630	−1.508	−1.128	0.276	−0.626	0.822	−0.517	2.344	
3	−0.519	−1.052	0.747	−0.550	−0.447	−0.993	1.031	0.242	1.499	
4	−1.257	0.389	−0.288	−0.427	−0.205	−0.772	−1.353	−0.665	−1.242	
5	−1.509	−2.458	1.153	−2.746	0.157	2.890	−0.370	0.090	1.079	
6	0.510	0.854	−1.891	0.208	0.169	1.187	−0.358	2.248	−0.451	
7	−0.300	−0.694	0.241	−0.540	1.734	−0.187	0.847	0.801	0.7920	
8	−0.705	0.214	−0.931	−1.016	−1.403	−0.359	0.972	1.827	1.144	
9	−1.746	0.027	−0.738	1.117	1.021	−0.144	0.201	0.396	−0.896	
10	−0.671	0.984	−0.003	0.466	0.470	−1.024	−0.600	1.919	2.002	
11	−1.230	−0.921	0.520	1.070	−0.330	1.598	0.794	−1.194	−1.312	
12	1.618	1.250	−0.681	−1.523	0.612	1.364	0.582	−1.480	−3.760	
13	−0.038	0.391	0.215	0.533	−1.187	−0.607	0.554	−0.598	−2.573	

Table 16
Weight and bias for different family II for fold K = 4.

Neurons	Weight to								Bias to	
	fck (MPa)	C (kg)	A (Kg)	W (kg)	FA (kg)	CA (kg)	SP (Kg)	% of RA	Layer 1	Layer 2
	Wi	W1	W2	W3	W4	W5	W6	W7	B1	B2
1	−0.398	2.779	−5.684	−4.831	−3.811	−0.601	−0.651	1.439	−3.325	1.113
2	−2.279	−0.529	−0.239	0.487	0.110	−2.973	0.281	0.533	0.798	
3	−1.504	−2.442	0.756	−0.897	−3.480	−1.993	0.390	−0.711	−1.678	
4	−0.316	2.025	6.258	−0.325	3.478	6.089	−5.056	−1.686	0.362	
5	−4.244	0.633	0.499	0.025	0.767	0.503	−0.013	−0.037	0.521	
6	0.702	5.273	−0.387	−0.217	1.468	3.086	7.290	−1.907	3.978	
7	1.970	1.474	1.654	−0.558	0.975	−1.394	0.312	0.591	0.928	
8	−0.634	1.564	3.664	−2.406	−2.795	4.039	3.492	1.151	3.639	
9	0.481	−4.806	3.062	5.072	12.584	7.316	−0.272	−0.088	−4.331	
10	0.817	−6.728	4.174	−1.787	−4.470	−4.427	−2.731	−2.511	−3.693	
11	−1.086	−1.510	−1.455	−0.458	−1.009	−0.340	0.872	0.782	−2.165	

strength from the ANN model and ANN-based equations for each family has R^2 as 1

To simplify the development of an equation based on the ANN model for each family, the equation is summarized from equation (3) to equation (6). C_{ij} is calculated from each family as multiplication of weight basis from Table 15 to Table 18 and input variables (normalized value) from Table 2. The summation of C_{ij} is taken for further calculation, which is nothing but multiple individual input variables and their corresponding input variable. b_{jh} is a bias to layer one from Table 15 to Table 18 for all families. A_j is calculated as the multiplication of weight of output variable and tan value of summation of C_{ij} and b_{jh}. A_j depends upon several neurons, and summation of it is considered along with bias to output layer for calculation of normalized value. The value is denormalized to calculate the predicted value of compressive strength.

$$f_{ck} = \left[Tanh\left\{ \sum_{1}^{n} (A_{ij}) + b_0 \right\} \right] \tag{3}$$

Table 17
Weight and bias for different family III for fold K = 10.

Neurons	Weight to								Bias to	
	fck (MPa)	C (kg)	A (Kg)	W (kg)	FA (kg)	CA (kg)	SP (Kg)	% of RA	Layer 1	Layer 2
	Wi	W1	W2	W3	W4	W5	W6	W7	B1	B2
1	−1.907	−1.745	−0.219	−0.713	−1.037	1.124	−0.384	0.424	2.477	−0.276
2	2.203	−2.140	1.274	−0.135	2.092	−0.462	2.516	0.388	−2.340	
3	−1.706	−0.412	0.678	0.349	−0.848	1.362	−0.655	−1.079	0.975	
4	1.560	−1.304	0.755	−0.751	−1.760	−0.742	0.955	−0.907	0.293	
5	1.571	−2.288	0.971	0.960	0.290	0.302	0.583	0.025	1.660	
6	−1.328	−1.671	−0.046	0.557	0.535	−0.998	0.639	−0.294	−0.316	
7	1.714	−0.197	−0.161	−0.787	−0.217	0.079	−2.651	0.209	−1.663	
8	1.229	1.057	−0.659	−0.390	−0.678	0.680	−0.672	0.263	0.234	
9	0.920	0.339	0.971	0.208	0.315	1.077	−1.625	−1.267	0.403	
10	0.535	−0.520	0.493	−1.019	−1.337	−0.727	1.892	1.953	1.755	
11	1.805	1.821	−1.533	0.170	0.580	−1.488	−1.053	0.036	1.482	
12	1.666	0.540	0.078	−0.312	−0.926	0.148	1.257	−2.385	3.778	

Table 18
Weight and bias for different family IV for fold K = 1.

Neurons	Weight to								Bias to	
	fck (MPa)	C (kg)	A (Kg)	W (kg)	FA (kg)	CA (kg)	SP (Kg)	% of RA	Layer 1	Layer 2
	Wi	W1	W2	W3	W4	W5	W6	W7	B1	B2
1	−0.404	−2.266	−0.042	−0.820	3.620	5.910	−3.733	0.724	0.335	0.251
2	−0.126	5.238	9.420	4.904	8.942	4.468	−2.159	2.475	2.114	
3	1.362	−1.963	1.396	−4.783	−1.073	0.457	3.133	−0.210	0.131	
4	3.032	−0.902	2.514	−0.221	−1.894	−0.249	−1.083	−0.007	1.305	
5	3.895	1.172	−1.568	−0.107	1.450	0.362	0.603	0.029	−0.902	
6	0.590	−6.243	−0.149	2.644	−0.709	−1.643	3.656	−0.277	2.627	
7	0.500	−11.837	0.057	3.873	9.693	2.578	7.235	−1.668	−6.391	
8	1.640	3.313	−0.038	3.346	1.804	0.483	−3.322	0.197	−0.114	
9	−0.337	−4.625	−0.840	4.039	6.982	−0.826	3.866	0.250	−1.213	

$$A_j = W_j x D_j \tag{4}$$

$$D_j = Tanh\left\{\left(\sum_{1}^{n} C_{ij}\right) + b_{jh}\right\} \tag{5}$$

$$C_{ij} = \left[X_i x W_{ij}\right] \tag{6}$$

W_{ij} is the connection weight of i^{th} input variable for j^{th} neuron; X_i is the regularized input element variable i. C_{ij} is the constant variable for multiplication of i^{th} input variable and j_{th} neuron, W_j is the connection weight between the j^{th} neuron and single output variable, and b_{jh} is the bias of j^{th} neuron of h^{th} hidden layer. A_j is the jth neuron's constant variable, and b_0 is the bias at the output layer. In this research's projected mathematical model for predicting artificial neural networks, the normalized input variables are seven, the target variable is one, the number of neurons connecting the input and concealed layers is found from literature, and the transfer function adopted is tan-sigmoid. Ahmed et al., 2019 [114] developed an ANN equation based on the penetration rate in deep shale formation and obtained a better R^2 value.

3.8. Sensitivity analysis using weight partitioning method

The weight partitioning method (WPM), which is used to unlock the black-box nature of the artificial neural network model Garson (1991) [115] and Goh (1995) [116], is assumed. WPM is a technique of partitioning the network weights to estimate the significance of each input variable in the network [117]. The technique needs to divide the hidden and output connection weights of every concealed neuron into components related to every input neuron. The strength of every input variable on the projected value could hence be obtained utilizing the equation (7) as follows

$$Q_{ik} = \left[\frac{\sum_{j=1}^{n}\left\{\frac{|W_{ij}|}{\sum_{i=1}^{m}|W_{ij}|}\left|V_{jk}\right|\right\}}{\sum_{i=1}^{m}\left(\sum_{j=1}^{n}\left\{\frac{|W_{ij}|}{\sum_{i=1}^{m}|W_{ij}|}\left\lceil V_{jk}\right\rceil\right\}\right)}\right]*100\% \tag{7}$$

Where Q_{ik} signifies the percentage influence of the input variables on the output values, w_{ij} represents the weights amid the input neuron i (=1, 2, …, m) and the concealed neuron j (=1, 2, …, n). V_{jk} signifies the weights amid the second layer neuron j and the last layer neuron k (=1,2, …, l). The most equally distributed input parameters are family I, and unequally distributed input parameters in family IV are noted in Fig. 12. The most influencing input parameter is cement, as indicated in Fig. 12 and the least influencing input parameter is recycled aggregate. The relative influence of each variable on the SCC family group and variables are shown in Figs. 12 and 13. The lowest equally influenced input parameters are admixture and water. The highest equally affected input parameters are fine aggregate and superplasticizer.

Based on the weight partition method, one of the input variables has a more significant influence of more than 25 %, as noted by Jiang et al., 2021 [107].

3.9. Sensitivity analysis from ANN-based equation

Sensitivity analysis from the ANN-based equation for all four families is shown in Fig. 14 based on R^2. The equation derived from the ANN model for four families of SCC with recycled aggregate is necessary nowadays to reduce the negative impacts. Sensitive analysis of input parameters was carried out by consecutively substituting all values of every input in the 7D input space with a persistent value (nearer to zero in this study) [118]. In this way, the statistical behavior of the omitted inputs is reduced to zero, permitting the forecast models to calculate the

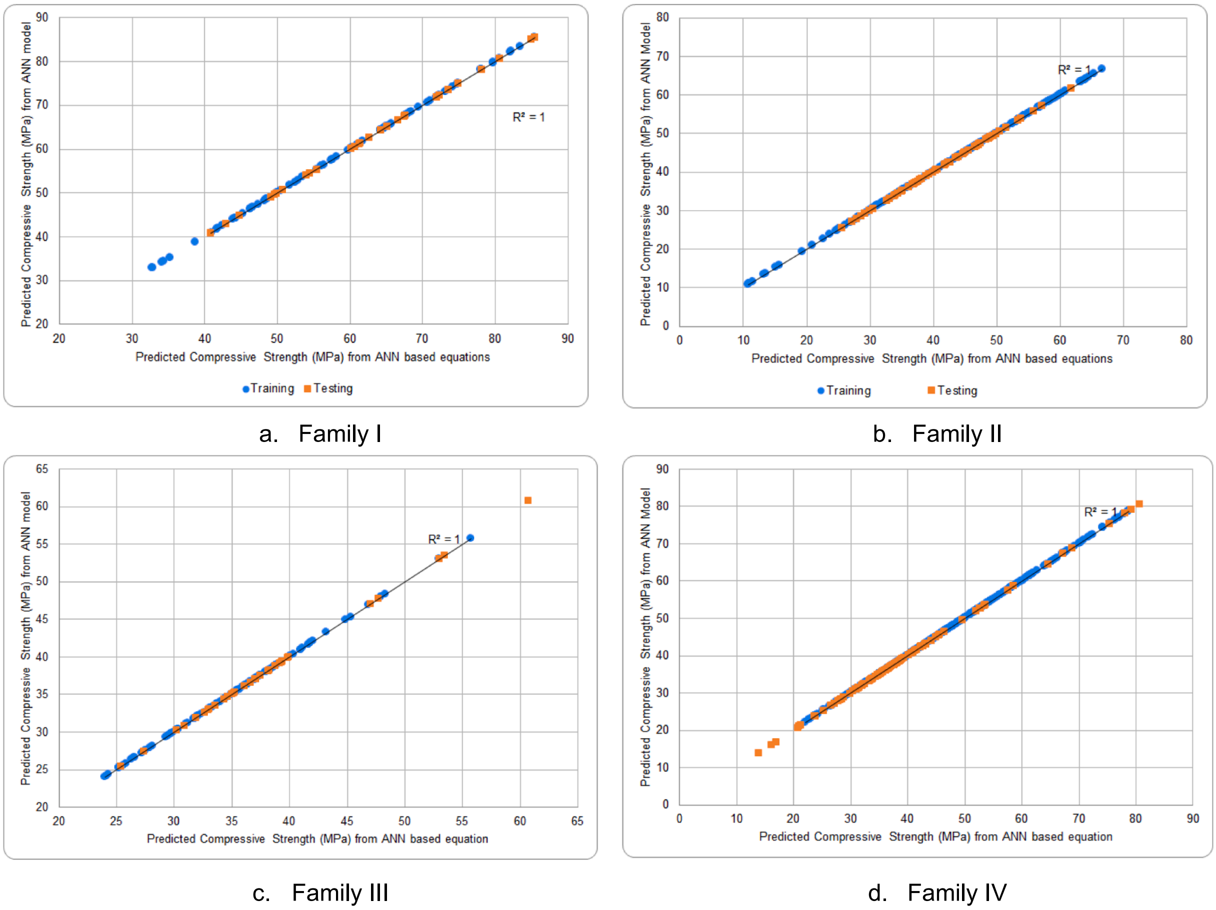

Fig. 11. Predicted compressive strength from ANN-based equation and ANN model.

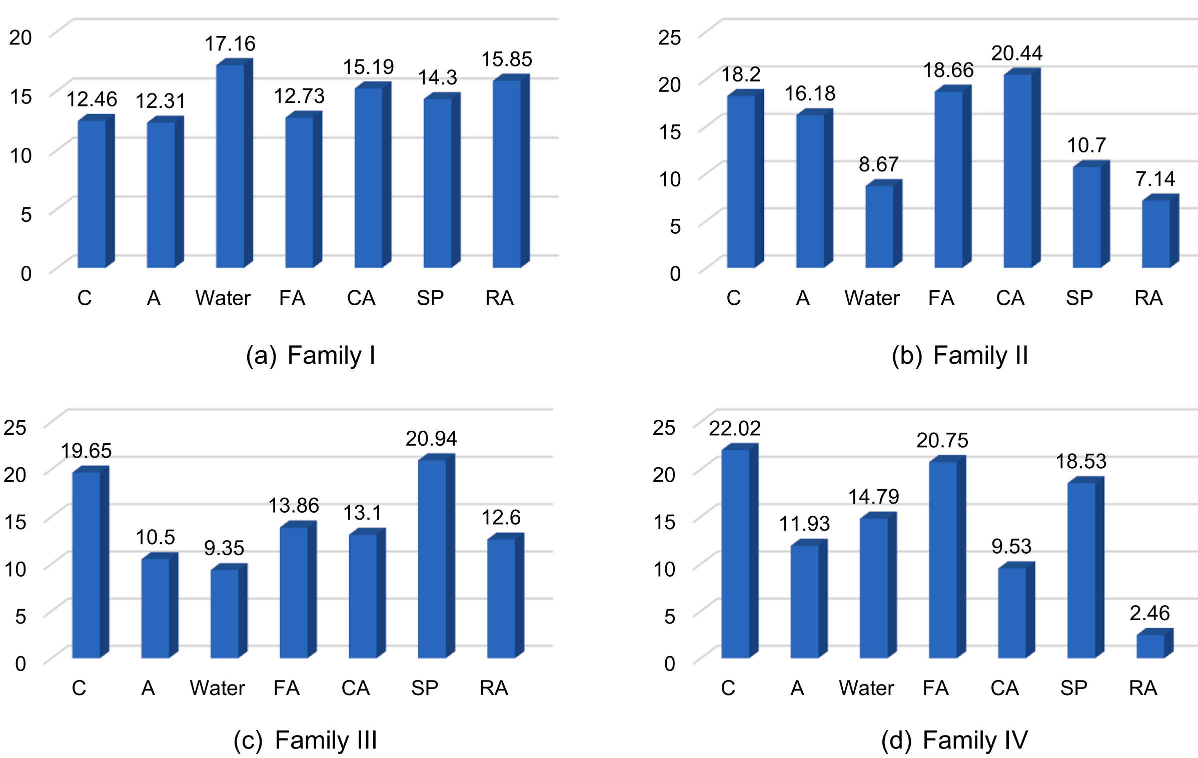

Fig. 12. Sensitivity analysis of each family from SCC with RA.

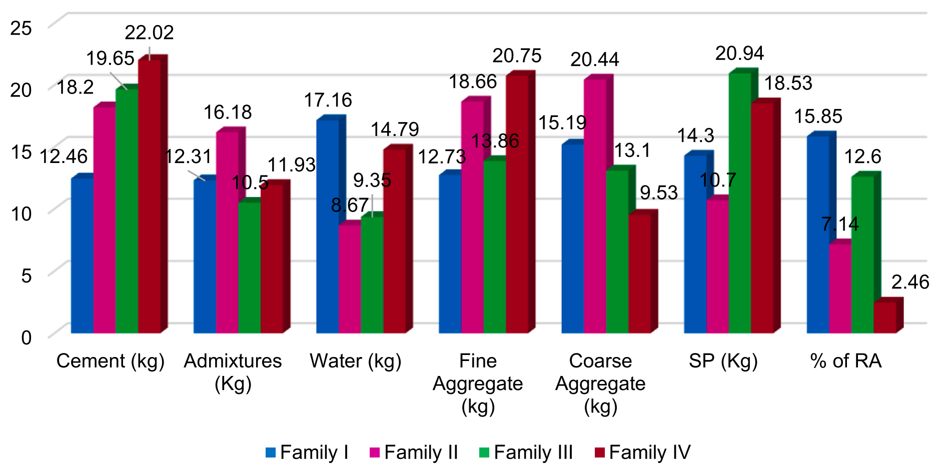

Fig. 13. Sensitivity analysis of the input parameters of SCC with RA.

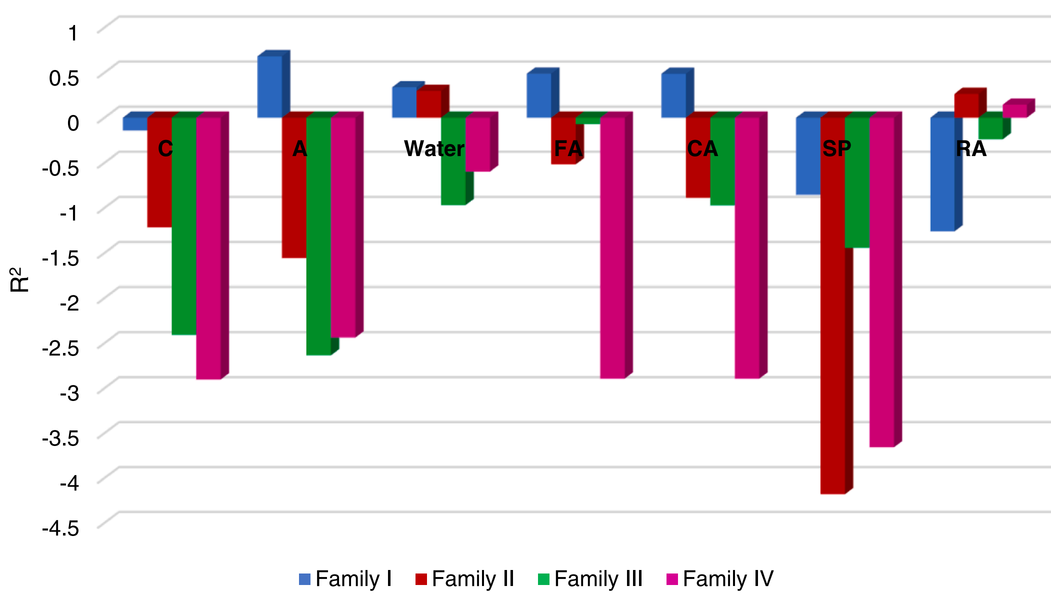

Fig. 14. Sensitivity analysis of the input parameters from ANN-based equations.

impact of this input data on the projected targets, even in the case of highly nonlinear relationships [118]. Lastly, the sensitivity index of inputs was attained by determining the difference of considered quality evaluation conditions between the point of full simulation and the case without an input [118].

It is also required to understand the impact of each input parameter (Cement, Admixtures, water, fine aggregate, coarse aggregate, superplasticizer, and recycled aggregate) on these equations. Positive and negative types of impacts are observed for all the input parameters, as noted in Fig. 15. The most negative influencing input parameter irrespective of the SCC family is monitored as a superplasticizer. Positive impacts are mainly observed for the input parameters water and recycled aggregate. Similarly, most negative effects are observed for the input parameters cement and superplasticizer. The influence of different input parameters for other families based on the R^2 value is shown in Fig. 15. Similar to input parameters, the families also negatively and positively impact the equation proposed from the ANN model. A positive impact is noted for the family I and family II, and a negative one is observed for families III and IV. Only family III has an entirely negative impact on the equation proposed from the ANN model, whereas all other families have both negative and positive effects. The most negatively influenced SCC family noted is family IV. The superplasticizer is the most influencing input parameter for families II and IV.

4. Conclusions

The study has examined how different statistical techniques from different tools can be utilized to anticipate the compression strength of self-consolidating concrete with recycled coarse aggregates based on its mix proportion. The goal is to enhance the concrete mixture design, quality control, and quality assurance. Drawing upon the findings of the research, the subsequent key outcomes can be deduced:

- The number of layers and the R^2 value for all families is no constant relationship is observed. No continuous relationship between the number of neurons and the R^2 value for all families is observed.
- R^2 value differs with different grades of families. It is noted that each family has its model depending on its compressive strength.
- K fold method is used to determine the optimum R^2 value for each family of SCC with recycled aggregate.
- A standard model equation for all families is developed for SCC with recycled aggregate based on ANN.

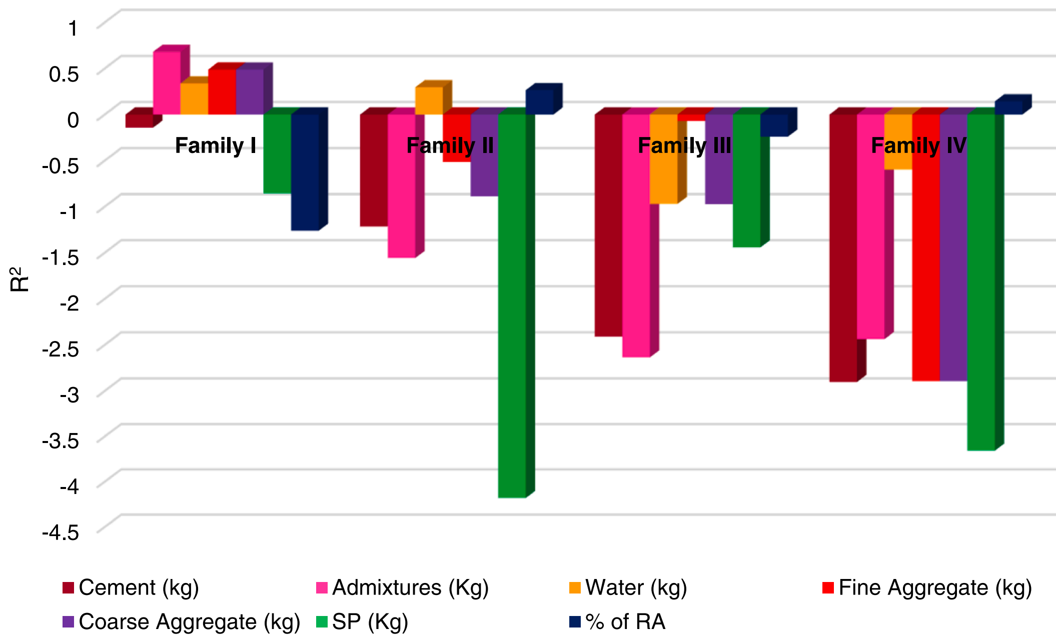

Fig. 15. Sensitivity analysis of the SCC with recycled aggregate families from ANN-based equations.

- Sensitivity analysis using the weight partition method shows that the most influenced input parameter is cement, and family I am the most equally affected family.
- Sensitivity analysis from an ANN-based equation shows that the most influenced input parameter is a superplasticizer, and the most affected family is family IV.

The results of the present research can help in developing a uniform soft tool for computing to project the compression strength of self-compacting recycled aggregate concrete accurately. When such a method is fully developed, the projection method could decrease the required time and cost for lab testing. The drawback of the present research can be in the range of the database's output and input. Thus, these ranges might restrain the model adaptability of artificial neuron networks and the numerical method in constituents of self-compacting concrete.

Declaration of Competing Interest

The authors declare that they have no known competing financial interests or personal relationships that could have appeared to influence the work reported in this paper.

Acknowledgment

Not applicable.

Funding resources

Not applicable.

References

[1] Chakkamalayath J, Joseph A, Al-Baghli H, et al. Performance evaluation of self-compacting concrete containing volcanic ash and recycled coarse aggregates. Asian J Civ Eng 2020;21:815–27. https://doi.org/10.1007/S42107-020-00242-2.
[2] Althoey F, Zaid O, de-Prado-Gil J, et al.Impact of sulfate activation of rice husk ash on the performance of high strength steel fiber reinforced recycled aggregate concrete. J Build Eng 2022;54:104610. 10.1016/j.jobe.2022.104610.
[3] Zaid O, Mukhtar FM, M-García R, et al. Characteristics of high-performance steel fiber reinforced recycled aggregate concrete utilizing mineral filler. Case Stud Constr Mater 2022;16. https://doi.org/10.1016/j.cscm.2022.e00939.
[4] Ahmad J, Zaid O, Aslam F, et al. A Study on the Mechanical Characteristics of Glass and Nylon Fiber Reinforced Peach Shell Lightweight Concrete. Materials (Basel) 2021;14:21–41. https://doi.org/10.3390/ma14164488.
[5] Zaid O, Ahmad J, Siddique MS, et al. A step towards sustainable glass fiber reinforced concrete utilizing silica fume and waste coconut shell aggregate. Sci Rep 2021;11:1–14.
[6] Ahmad J, Zaid O, Pérez C-L-C, et al. Experimental Research on Mechanical and Permeability Properties of Nylon Fiber Reinforced Recycled Aggregate Concrete with Mineral Admixture. Appl Sci 2022;12. https://doi.org/10.3390/app12020554.
[7] Zaid O, Martínez-García R, Abadel AA, et al. To determine the performance of metakaolin-based fiber-reinforced geopolymer concrete with recycled aggregates. Arch Civ Mech Eng 2022;22:114. https://doi.org/10.1007/s43452-022-00436-2.
[8] Zaid O, Zamir Hashmi SR, Aslam F, Alabduljabbar H. Experimental Study on Mechanical Performance of Recycled Fine Aggregate Concrete Reinforced With Discarded Carbon Fibers. Front Mater 2021;8:481. https://doi.org/10.3389/fmats.2021.771423.
[9] Zhao Y, Wang S, Zhang Z, et al. Driving factors of carbon emissions embodied in China-US trade: A structural decomposition analysis. J Clean Prod 2016;131:678–89. https://doi.org/10.1016/J.JCLEPRO.2016.04.114.
[10] Smirnova OM, de Navascués I, Mikhailevskii VR, et al. Sound-Absorbing Composites with Rubber Crumb from Used Tires. Appl Sci 2021;11. https://doi.org/10.3390/app11167347.
[11] Smirnova O, Kazanskaya L, Koplík J, et al. Concrete Based on Clinker-Free Cement: Selecting the Functional Unit for Environmental Assessment. Sustainability 2021;13. https://doi.org/10.3390/su13010135.
[12] Yakovlev G, Полянских И, Gordina A, et al. Influence of Sulphate Attack on Properties of Modified Cement Composites. Appl Sci 2021;11:8509. https://doi.org/10.3390/app11188509.
[13] Smirnova O, Menéndez-Pidal I, Alekseev A, et al. Strain Hardening of Polypropylene Microfiber Reinforced Composite Based on Alkali-Activated Slag Matrix. Materials (Basel) 2022;15:1607. https://doi.org/10.3390/ma15041607.
[14] Saidova Z, Yakovlev G, Smirnova O, et al. Modification of Cement Matrix with Complex Additive Based on Chrysotyl Nanofibers and Carbon Black. Appl Sci 2021;11:6943. https://doi.org/10.3390/app11156943.
[15] Smirnova O. Development of classification of rheologically active microfillers for disperse systems with Portland cement and superplasticizer. Int J Civ Eng Technol 2018;9:1966–73.
[16] Faraj RH, Sherwani AFH, Draei K. Mechanical, fracture and durability properties of self-compacting high strength concrete containing recycled polypropylene plastic particles. Journal of Building engineering 2019;25:100808. https://doi.org/10.1016/j.jobe.2019.100808.
[17] Athiyamaan V, Mohan Ganesh G. Analysis of the alignment of micro-steel fibers in admixture- based self-compacting concrete (MSFR-SCC) using NDT and evaluation of its effect on the modulus of rupture. Int J Technol 2019;10:5–15. https://doi.org/10.14716/IJTECH.V10I1.2066.
[18] Pazouki G, Pourghorban A. Using a hybrid artificial intelligence method for estimating the compressive strength of recycled aggregate self compacting concrete. Eur J Environ Civ Eng 2021. https://doi.org/10.1080/19648189.2021.1908915.

[19] Saha P, Prasad MLV, Rathish Kumar P. Predicting strength of SCC using artificial neural network and multivariable regression analysis. Comput Concr 2017;20(1): 031–8. https://doi.org/10.12989/cac.2017.20.1.031.

[20] Ji T, Lin T, Lin X. A concrete mix proportion design algorithm based on artificial neural networks. undefined 2006;36:1399–1408. 10.1016/J.CEMCONRES.2006.01.009.

[21] Ni HG, Wang JZ. Prediction of compressive strength of concrete by neural networks. Cem Concr Res 2000;30:1245–50. https://doi.org/10.1016/S0008-8846(00)00345-8.

[22] Abu Yaman M, Abd Elaty M, Taman M. Predicting the ingredients of self compacting concrete using artificial neural network. Alexandria Eng J 2017;56: 523–32. https://doi.org/10.1016/J.AEJ.2017.04.007.

[23] Tavakoli HR, Omran OL, Shiade MF, Kutanaei SS. Prediction of combined effects of fibers and nanosilica on the mechanical properties of self-compacting concrete using artificial neural network. Lat Am J Solids Struct 2014;11:1906–23. https://doi.org/10.1590/S1679-78252014001100002.

[24] Wu X, Ghaboussi J, Garrett JH. Use of neural networks in detection of structural damage. Comput Struct 1992;42:649–59. https://doi.org/10.1016/0045-7949(92)90132-J.

[25] Hossain KMA, Lachemi M, Easa SM. Artificial neural network model for the strength prediction of fully restrained RC slabs subjected to membrane action. Comput Concr 2006;3:439–54. https://doi.org/10.12989/CAC.2006.3.6.439.

[26] Ghaboussi J, GarrettJr JH, Wu X. KnowledgeBased Modeling of Material Behavior with Neural Networks. J Eng Mech 1991;117:132–53. https://doi.org/10.1061/(ASCE)0733-9399(1991)117:1(132).

[27] El-Chabib H, Nehdi M, Sonebi M. Artificial intelligence model for flowable concrete mixtures used in underwater construction and repair. ACI Mater J 2003;100.

[28] Salciccioli JD, Crutain Y, Komorowski M, Marshall DC. Sensitivity Analysis and Model Validation. Second Anal Electron Heal Rec 2016;263–271. https://doi.org/10.1007/978-3-319-43742-2_17.

[29] Boudali S, Abdulsalam B, Rafiean AH, Poncet S, Soliman A, Elsafty A. Influence of fine recycled concrete powder on the compressive strength of self-compacting concrete using artificial neural network. Sustainability 2021;13:3111. https://doi.org/10.3390/su13063111.

[30] Asteris PG, Kolovos KG, Douvika MG, Roinos K. Prediction of self-compacting concrete strength using artificial neural networks. Eur J Environ Civ Eng 2016;20(1):102–22. https://doi.org/10.1080/19648189.2016.1246693.

[31] Morales DS, Morera LS, Jimenez JR, Hernandez LG. A novel artificial neural network to predict the compressive strength of recycled aggregate concrete. Appl Sci 2021;11:11077. https://doi.org/10.3390/app112211077.

[32] Vasanthalin CP, Kavitha CN. Prediction of compressive strength of recycled aggregate concrete using artificial neural network and cuckoo search method. Mater Today: Proc 2021. https://doi.org/10.1016/j.matpr.2021.03.500.

[33] Ridho MABKA, Ngamkhanong C, Wu Y, Kaewunruen S. Recycled aggregates concrete compressive strength prediction using artificial neural networks. Infra structures 2021;6:17. https://doi.org/10.3390/infrastructures6020017.

[34] Saleh HM, Rahman OA. Introductory Chapter: Properties and applications of cement-based materials. Cement Based Mater 2018;1–12. https://doi.org/10.5772/intechopen.73784.

[35] Mazloom M, Salehi H. The relationship between fracture toughness and compressive strength of self-compacting light weight concrete. IOP Conf Series: Mater Sci Eng 2018;431(6):062007. https://10.1088/1757-899X/431/6/062007.

[36] Salehi M, Mazloom M. Effect of magnetic field intensity on fracture behaviours of self-compacting lightweight concrete. Mag Concr Res 2019;71(3):665–79. https://doi.org/10.1680/jmacr.17.00418.

[37] Afzali-Naniz O, Mazloom M, Karamloo M. Effect of nano and micro SIO2 on brittleness and fracture parameters of self-compacting lightweight concrete. Constr Build Mater 2021;299:124354. https://doi.org/10.1016/j.conbuildmat.2021.124354.

[38] Khademi F, Jamal SM, Deshpande N, Londhe S. Predicting strength of recycled aggregate concrete using Artificial Neural Network, Adaptive Neuro-Fuzzy Inference System and Multiple Linear Regression. Int J Sustain Built Environ 2016;5:355–69. https://doi.org/10.1016/J.IJSBE.2016.09.003.

[39] Huang X, Zhang J, Sresakoolchai J, Kaewunruen S. Machine Learning Aided Design and Prediction of Environmentally Friendly Rubberised Concrete. Sustain 2021, Vol 13, Page 1691 13:1691. 10.3390/SU13041691.

[40] Gesoglu M, Güneyisi E, Öz HÖ, et al. Failure characteristics of self-compacting concretes made with recycled aggregates. Constr Build Mater 2015;98:334–44. https://doi.org/10.1016/j.conbuildmat.2015.08.036.

[41] Wang J, Dai Q, Si R, et al. Fresh and mechanical performance and freeze-thaw durability of steel fiber-reinforced rubber self-compacting concrete (SRSCC). J Clean Prod 2020;277:123180. https://doi.org/10.1016/j.jclepro.2020.123180.

[42] Sadeghi-Nik A, Berenjian J, Alimohammadi S, et al. The Effect of Recycled Concrete Aggregates and Metakaolin on the Mechanical Properties of Self-Compacting Concrete Containing Nanoparticles. Iran J Sci Technol - Trans Civ Eng 2019;43:503–15. https://doi.org/10.1007/s40996-018-0182-4.

[43] Khafaga SA. Production of High Strength Self Compacting Concrete Using Recycled Concrete as Fine and/or Coarse Aggregates. World Appl Sci J 2014;29: 465–74. https://doi.org/10.5829/idosi.wasj.2014.29.04.13861.

[44] Revilla-Cuesta V, Ortega-López V, Skaf M, Manso JM. Effect of fine recycled concrete aggregate on the mechanical behavior of self-compacting concrete. Constr Build Mater 2020;263:120671. https://doi.org/10.1016/j.conbuildmat.2020.120671.

[45] Fiol F, Thomas C, Muñoz C, et al. The influence of recycled aggregates from precast elements on the mechanical properties of structural self-compacting concrete. Constr Build Mater 2018;182:309–23. https://doi.org/10.1016/j.conbuildmat.2018.06.132.

[46] Behera M, Minocha AK, Bhattacharyya SK. Flow behavior, microstructure, strength and shrinkage properties of self-compacting concrete incorporating recycled fine aggregate. Constr Build Mater 2019;228:116819. https://doi.org/10.1016/j.conbuildmat.2019.116819.

[47] Ali EE, Al-Tersawy SH. Recycled glass as a partial replacement for fine aggregate in self compacting concrete. Constr Build Mater 2012;35:785–91. https://doi.org/10.1016/J.CONBUILDMAT.2012.04.117.

[48] Señas L, Priano C, Marfil S. Influence of recycled aggregates on properties of self-consolidating concretes. Constr Build Mater 2016;113:498–505. https://doi.org/10.1016/j.conbuildmat.2016.03.079.

[49] Aslani F, Ma G, Yim Wan DL, Muselin G. Development of high-performance self-compacting concrete using waste recycled concrete aggregates and rubber granules. J Clean Prod 2018;182:553–66. https://doi.org/10.1016/j.jclepro.2018.02.074.

[50] Uygunoǩlu T, Topçu IB, Çelik AG. Use of waste marble and recycled aggregates in self-compacting concrete for environmental sustainability. J Clean Prod 2014;84: 691–700. https://doi.org/10.1016/j.jclepro.2014.06.019.

[51] Kou SC, Poon CS. Properties of self-compacting concrete prepared with coarse and fine recycled concrete aggregates. Cem Concr Compos 2009;31:622–7. https://doi.org/10.1016/j.cemconcomp.2009.06.005.

[52] Grdic ZJ, Toplicic-Curcic GA, Despotovic IM, Ristic NS. Properties of self-compacting concrete prepared with coarse recycled concrete aggregate. Constr Build Mater 2010;24:1129–33. https://doi.org/10.1016/j.conbuildmat.2009.12.029.

[53] Tang WC, Ryan PC, Cui HZ, Liao W. Properties of Self-Compacting Concrete with Recycled Coarse Aggregate. Adv Mater Sci Eng 2016;2016. https://doi.org/10.1155/2016/2761294.

[54] Tuyan M, Mardani-aghabaglou A, Ramyar K. Freeze – thaw resistance, mechanical and transport properties of self-consolidating concrete incorporating coarse recycled concrete aggregate. Mater Des 2014;53:983–91. https://doi.org/10.1016/j.matdes.2013.07.100.

[55] Güneyisi E, Gesoglu M, Algın Z, Yazıcı H. Effect of surface treatment methods on the properties of self-compacting concrete with recycled aggregates. Constr Build Mater 2014;64:172–83.

[56] Yu JJ, Gong J, Zou JM, Yang WK. Study on Properties of Self-Compacting Concrete Prepared with Coarse Recycled Concrete Aggregate. Appl Mech Mater 2014;638–640:1494–8. https://doi.org/10.4028/WWW.SCIENTIFIC.NET/AMM.638-640.1494.

[57] Zhou AG, Yin J, Song WM, Chi Y. Research on Self-Compacting Concrete Made with Recycled Aggregate. Adv Mater Res 2013;639–640:399–403. https://doi.org/10.4028/WWW.SCIENTIFIC.NET/AMR.639-640.399.

[58] Guo Z, Jiang T, Zhang J, et al. Mechanical and durability properties of sustainable self-compacting concrete with recycled concrete aggregate and fly ash, slag and silica fume. Constr Build Mater 2020;231:117115. https://doi.org/10.1016/j.conbuildmat.2019.117115.

[59] Siva S, Krishna R, Sowjanya Vani V, et al. Studies on Mechanical Properties of Ternary Blended Self-Compacting Concrete Using Different Percentages of Recycled Aggregate. Int J Civ Eng Technol (IJCIET 2018;9:1672–80.

[60] Khodair Y, Luqman. Self-compacting concrete using recycled asphalt pavement and recycled concrete aggregate. J Build Eng 2017;12:282–7. https://doi.org/10.1016/j.jobe.2017.06.007.

[61] Katar I, Ibrahim Y, Malik MA, Khahro SH.Mechanical Properties of Concrete with Recycled Concrete Aggregate and Fly Ash. Recycl 2021, Vol 6, Page 23 6:23. 10.3390/RECYCLING6020023.

[62] Martínez-García R, Guerra-Romero IM, Morán-del Pozo JM, et al. Recycling aggregates for self-compacting concrete production: A feasible option. Materials (Basel) 2020;13. https://doi.org/10.3390/ma13040868.

[63] Duan Z, Singh A, Xiao J, Hou S. Combined use of recycled powder and recycled coarse aggregate derived from construction and demolition waste in self-compacting concrete. Constr Build Mater 2020;254:119323. https://doi.org/10.1016/j.conbuildmat.2020.119323.

[64] Pan Z, Zhou J, Jiang X, et al. Investigating the effects of steel slag powder on the properties of self-compacting concrete with recycled aggregates. Constr Build Mater 2019;200:570–7. https://doi.org/10.1016/j.conbuildmat.2018.12.150.

[65] Manzi S, Mazzotti C, Bignozzi MC. Self-compacting concrete with recycled concrete aggregate: Study of the long-term properties. Constr Build Mater 2017;157:582–90. https://doi.org/10.1016/j.conbuildmat.2017.09.129.

[66] Nili M, Sasanipour H, Aslani F. The Effect of Fine and Coarse Recycled Aggregates on Fresh and Mechanical Properties of Self-Compacting Concrete. Materials (Basel) 2019;12:1120. https://doi.org/10.3390/ma12071120.

[67] Singh A, Arora S, Sharma V, Bhardwaj B. Workability Retention and Strength Development of Self-Compacting Recycled Aggregate Concrete Using Ultrafine Recycled Powders and Silica Fume. J Hazardous, Toxic, Radioact Waste 2019;23: 04019016. https://doi.org/10.1061/(ASCE)HZ.2153-5515.0000456.

[68] Vinay Kumar BM, Ananthan H, Balaji KVA. Experimental studies on utilization of coarse and finer fractions of recycled concrete aggregates in self compacting concrete mixes. J Build Eng 2017;9:100–8. https://doi.org/10.1016/J.JOBE.2016.11.013.

[69] Sharifi Y, Houshiar M, Aghebati B. Recycled glass replacement as fine aggregate in self-compacting concrete. Front Struct Civ Eng 2013;7:419–28. https://doi.org/10.1007/s11709-013-0224-8.

[70] Mahakavi P, Chithra R. Effect of recycled coarse aggregate and manufactured sand in self compacting concrete; 2019. 10.1080/13287982.2019.1636519.
[71] Bahrami N, Zohrabi M, Mahmoudy SA, Akbari M. Optimum recycled concrete aggregate and micro-silica content in self-compacting concrete: Rheological, mechanical and microstructural properties. J Build Eng 2020;31:101361. https://doi.org/10.1016/j.jobe.2020.101361.
[72] Silva P, de Brito J. Experimental study of the mechanical properties and shrinkage of self-compacting concrete with binary and ternary mixes of fly ash and limestone filler. Eur J Environ Civ Eng 2017;21:430–53. https://doi.org/10.1080/19648189.2015.1131200.
[73] Sun C, Chen Q, Xiao J, Liu W. Resources, Conservation & Recycling Utilization of waste concrete recycling materials in self-compacting concrete. Resour Conserv Recycl 2020;161:104930. https://doi.org/10.1016/j.resconrec.2020.104930.
[74] Surendar M, Beulah Gnana Ananthi G, Sharaniya M, et al. Mechanical properties of concrete with recycled aggregate and M−sand. Mater Today Proc 2021;44:1723–30. https://doi.org/10.1016/j.matpr.2020.11.896.
[75] Babalolaa OE, Awoyera PO, Tran MT, et al (2020) Mechanical and durability properties of recycled aggregate concrete with ternary binder system and optimized mix proportion. 9:6521–6532. 10.1016/j.jmrt.2020.04.038.
[76] Nieto D, Dapena E, Alaejos P, et al. Properties of Self-Compacting Concrete Prepared with Coarse Recycled Concrete Aggregates and Different Water: Cement Ratios. J Mater Civ Eng 2019;31:04018376. https://doi.org/10.1061/(ASCE)MT.1943-5533.0002566.
[77] Revathi P, Selvi RS, Velin SS. Investigations on fresh and hardened properties of recycled aggregate self-compacting concrete. J Inst Eng India Ser A 2013;94(3):179–85. https://doi.org/10.1007/s40030-014-0051-5.
[78] Thomas C, Setién J, Polanco JA. Structural recycled aggregate concrete made with precast wastes. Constr Build Mater 2016;114:536–46. https://doi.org/10.1016/J.CONBUILDMAT.2016.03.203.
[79] Almeida Filho FM, Barragán BE, Casas JR, El Debs ALHC. Hardened properties of self-compacting concrete — A statistical approach. Constr Build Mater 2010;24:1608–15. https://doi.org/10.1016/J.CONBUILDMAT.2010.02.032.
[80] Malik AK, Gao R, Ganaie MA, Tanveer M, Suganthan PN. Random vector functional link network: recent developments, applications and future directions. Appl Soft Comput 2023;143:110377. https://doi.org/10.1016/j.asoc.2023.110377.
[81] de-Prado-Gil J, Palencia C, Jagadesh P, Martinez-Garcia, (2022) A study on the prediction of compressive strength of self-compacting recycled aggregate concrete utilizing novel computational approaches. Materials 15(15):5232. 10.3390/ma15155232.
[82] Ozkilic YO, Zeybek O, Bahrami A, Celik AI, Mydin MAO, Karalar M, et al. Optimum usage of waste marble powder to reduce use of cement toward eco-friendly concrete. J Mater Researcha Technol 2023;25:4799–819. https://doi.org/10.1016/j.jmrt.2023.06.126.
[83] Lawal AI, Aladejare AE, Onifade M, et al. Predictions of elemental composition of coal and biomass from their proximate analyses using ANFIS, ANN and MLR. Int J Coal Sci Technol 2021;8:124–40. https://doi.org/10.1007/S40789-020-00346-9/FIGURES/11.
[84] Fausett LV. Fundamentals of neural networks : architectures, algorithms, and applications. 1994;461.
[85] Neville AM. Properties of concrete. 1981;779.
[86] Hush DR. Classification with neural networks: A performance analysis. 1989; 277–280. 10.1109/ICSYSE.1989.48672.
[87] Popovics S. Analysis of Concrete Strength Versus Water-Cement Ratio Relationship. Mater J 1990;87(517–529).
[88] Gallant SI Neural Network Learning and Expert Systems.
[89] Wang C. A theory of generalization in learning machines with neural network applications. Diss available from ProQuest; 1994.
[90] Masters T, New SD, Boston Y Practical Neural Network Recipes in C++.
[91] Li JY, Chow TWS, Yu YL. Estimation theory and optimization algorithm for the number of hidden units in the higher-order feedforward neural network. IEEE Int Conf Neural Networks - Conf Proc 1995;3:1229–33. https://doi.org/10.1109/ICNN.1995.487330.
[92] Tamura S, Tateishi M. Capabilities of a four-layered feedforward neural network: Four layers versus three. IEEE Trans Neural Networks 1997;8:251–5. https://doi.org/10.1109/72.557662.
[93] Lai S, Serra M. Concrete strength prediction by means of neural network. Constr Build Mater 1997;11:93–8. https://doi.org/10.1016/S0950-0618(97)00007-X.
[94] Nagendra S. Practical Aspects of Using Neural Networks: Necessary Preliminary Specifications. GE Res Dev Cent Tech Inf Ser; 1997.
[95] Zhang Z, Ma X, Yang Y. Bounds on the number of hidden neurons in three-layer binary neural networks. Neural Netw 2003;16:995–1002. https://doi.org/10.1016/S0893-6080(03)00006-6.
[96] Shibata K. Effect of number of hidden neurons on learning in large-scale layered neural networks; 2009.
[97] Sheela KG, Deepa SN. Review on methods to fix number of hidden neurons in neural networks. Math Probl Eng 2013;2013. https://doi.org/10.1155/2013/425740.
[98] Hunter D, Hao Y, Pukish MS, et al. Selection of Proper Neural Network Sizes and Architectures-A Comparative Study; 2012. 10.1109/TII.2012.2187914.
[99] Ripely. Networks and Chaos—Statistical and Probabilistic Aspects. 2012;36: 435–435. https://doi.org/101080/00401706199410485870.
[100] Paola JD, Schowengerdt RA The Effect of Neural-Network Structure on a Multispectral Land-Use/Land-Cover Classification.
[101] Singh WR, Jain MK. Continuous hydrological modeling using soil moisture accounting algorithm in Vamsadhara river basin, India. J Water Resource Hydraulic Eng 2015;4(4):398–408.
[102] Keleştemur O, Arici E, Yildiz S, Gökçer B. Performance evaluation of cement mortars containing marble dust and glass fiber exposed to high temperature by using Taguchi method. Constr Build Mater 2014;60:17–24. https://doi.org/10.1016/J.CONBUILDMAT.2014.02.061.
[103] Al-Swaidani AM, Khwies WT. Applicability of Artificial Neural Networks to Predict Mechanical and Permeability Properties of Volcanic Scoria-Based Concrete. Adv Civ Eng 2018;2018. https://doi.org/10.1155/2018/5207962.
[104] Mashhadban H, Kutanaei SS, Sayarinejad MA. Prediction and modeling of mechanical properties in fiber reinforced self-compacting concrete using particle swarm optimization algorithm and artificial neural network. Constr Build Mater 2016;119:277–87. https://doi.org/10.1016/J.CONBUILDMAT.2016.05.034.
[105] Yeh IC. Modeling slump flow of concrete using second-order regressions and artificial neural networks. Cem Concr Compos 2007;29:474–80. https://doi.org/10.1016/J.CEMCONCOMP.2007.02.001.
[106] Goh ATC. Modeling Soil Correlations Using Neural Networks. J Comput Civ Eng 1995;9:275–8. https://doi.org/10.1061/(ASCE)0887-3801(1995)9:4(275).
[107] Jiang S, Sharafisafa M, Shen L. Using Artificial Neural Networks to Predict Influences of Heterogeneity on Rock Strength at Different Strain Rates. Mater 2021, Vol 14, Page 3042 14:3042. 10.3390/MA14113042.
[108] Aggarwal P, Aggarwal Y. Prediction of Compressive Strength of Self- Compacting Concrete with Fuzzy Logic. Int J Math Comput Sci 2011;5:774–81. https://doi.org/10.5281/ZENODO.1330501.
[109] Awoyera PO, Kirgiz MS, Viloria A, Ovallos-Gazabon D. Estimating strength properties of geopolymer self-compacting concrete using machine learning techniques. J Mater Res Technol 2020;9:9016–28. https://doi.org/10.1016/J.JMRT.2020.06.008.
[110] Uysal M, Tanyildizi H. Estimation of compressive strength of self compacting concrete containing polypropylene fiber and mineral additives exposed to high temperature using artificial neural network. Constr Build Mater 2012;27:404–14. https://doi.org/10.1016/J.CONBUILDMAT.2011.07.028.
[111] Prasad BKR, Eskandari H, Reddy BVV. Prediction of compressive strength of SCC and HPC with high volume fly ash using ANN. Constr Build Mater 2009;23:117–28. https://doi.org/10.1016/J.CONBUILDMAT.2008.01.014.
[112] Siddique R, Aggarwal P, Aggarwal Y. Prediction of compressive strength of self-compacting concrete containing bottom ash using artificial neural networks. Adv Eng Softw 2011;42:780–6. https://doi.org/10.1016/J.ADVENGSOFT.2011.05.016.
[113] Jagadesh P, de Prado-Gil J, Silva-Monteiro N, Martinez-Garcia R. Assessing the compressive strength of self-compacting concrete with recycled aggregates from mix ratio using machine learning approach. J Mater Res Technol 2023;24:1483–98. https://doi.org/10.1016/j.jmrt.2023.03.037.
[114] Ahmed A, Ali A, Elkatatny S, Abdulraheem A. New Artificial Neural Networks Model for Predicting Rate of Penetration in Deep Shale Formation. Sustain 2019, Vol 11, Page 6527 11:6527. 10.3390/SU11226527.
[115] Garson GD. Interpreting neural network connection weights. Artificial intellogence expert. 1991;6:46-51.
[116] Goh ATC. Back propagation neural networks for modeling complex systems. Artifiical intelligence in engineering 1995;9:143-151. 10.1016/0954-1810(94)00011-S.
[117] Mazloom M, Tajar SF, Mahboubi F. Long-term quality control of self-compacting semi-lightweight concrete using short-term compressive strength and combinatorial artifical neural networks. Computers and concrete 2020;25(5):401-409. 10/12989/cac.2020.25.5.401.
[118] Dao D Van, Adeli H, Ly H-B, et al. A Sensitivity and Robustness Analysis of GPR and ANN for High-Performance Concrete Compressive Strength Prediction Using a Monte Carlo Simulation. Sustain 2020, Vol 12, Page 830 12:830. 10.3390/SU12030830.

Rebeca Martínez-García (ORCID 0000-0002-8974-5759), Architect and Ph.D. in Biosystems Engineering. Professor at the University of León, among other topics in Graphic Expression in Engineering since 2013. Co-author of numerous articles in high impact scientific journals indexed in JCR, co-author in different international conferences and research projects, is member of the research unit Engineering of Materials and Eco-Efficiency (INMATECO). Director of project development and project management of more than 300 projects of Architecture and Engineering of new construction, rehabilitation, agro-industrial projects and public buildings.